Multimedia Tools and Applications
https://doi.org/10.1007/s11042-023-15494-8

Similarity detection method of science fiction painting based on multi-strategy improved sparrow search algorithm and Gaussian pyramid

Gang Chen[1] · **Donglin Zhu**[2] · **Xiangyu Chen**[1]

Received: 24 February 2022 / Revised: 4 September 2022 / Accepted: 18 April 2023

Abstract

Although image detection technology is widely used in various fields, there is still a large gap in the similarity detection of science fiction painting. Therefore, a similarity detection method for science fiction painting is proposed. Firstly, a k-layer pyramid image is created for the source image to be detected and the template image. Then, multi-strategy improved sparrow algorithm (MISSA) is used to perform rough matching in the top subgraph of the source image to obtain the coordinates of the initial matching target, the location transferred from the layer above each layer is the starting point of search, and pixel by pixel matching is carried out within the set window range. Finally, pHash is used as the similarity measure to calculate the similarity of matching results. The hybrid search strategy based on step function, multi-stage dynamic control of safety threshold, and food search strategy based on Logistic model are used to improve sparrow search algorithm, thereby forming MISSA to improve the accuracy and real-time performance in the matching process. In terms of performance verification of MISSA, the rationality and effectiveness of the three improved strategies are verified by ablation experiment, and the experimental results on CEC2017 benchmark function show that the optimization performance and convergence performance of MISSA are better than that of peer algorithms. The comparison results in the similarity detection experiment of science fiction painting fully verify that the proposed detection method has strong robustness in meeting the requirements of real-time and accuracy of matching.

Keywords Sparrow search algorithm · Gaussian pyramid · Multi-strategy improvements · Science fiction painting · Similarity detection

✉ Gang Chen
201127006@fzu.edu.cn

Extended author information available on the last page of the article.

Nomenclature

Variables

$x_{i,j}^t$, $x_{i,j}(t)$	position of the i-th producer in the j-dimensional search space at the t-th iteration
x_{worst}^t	current worst foraging position
x_p^{t+1}	position of the producer with the optimal fitness value at the t+1 iteration
x_{best}^t	current global optimal position
x_{rand}^t	a randomly selected sparrow individual
$\overline{x}_j(t)$	average position of the t-th generation population

Parameters

S	safety threshold
P	population size of sparrows
α	random number
Q	a random number that obeys a normal distribution
A	a column vector of the same dimension as the sparrow individual
f_i	fitness value of the current scout
f_g	global optimal fitness value
f_w	worst fitness value
β	a step-length control parameter that obeys the standard normal distribution
ε	a constant used to prevent the denominator from being zero
K	a random number
k_1, k_2	random numbers in (0, 1)
R_2	warning value
T_{max}	maximum number of iterations
L	a d-dimensional row vector with all elements 1
lb_i, ub_i	the lower and upper bounds of the control factor
T_i	the number of iterations in the i-th segment
a, b	expansion and translation factors
G	amplitude gain
w	control parameters of upper and lower bounds
D	dimension of optimization problem
N	population size of sparrow

Abbreviations

SSA	sparrow search algorithm
$MISSA$	multi-strategy improved sparrow search algorithm
GP	Gaussian pyramid
NCC	normalized cross-correlation
TM	template matching
GWO	gray wolf optimization algorithm
PSO	particle swarm optimization algorithm
WOA	whale optimization algorithm
ABC	artificial bee colony algorithm
$ISSA1$	improved sparrow search algorithm
$CSSA$	chaotic sparrow search algorithm
$ISSA2$	improved sparrow search algorithm
$pHash$	perceptual hash

1 Introduction

Modern society needs to give full play to subjectivity and creativity of everyone, and science fiction painting is a good way to cultivate personality and innovative thinking of students, and it is also one of the important ways to achieve scientific and technological quality education. Science fiction painting with rich colors and peculiar ideas has always been one of the focuses of the youth science and technology innovation competition. Good science fiction painting is referred to or imitated by many people. Nowadays, as people pay more and more attention to the protection of intellectual property rights, the importance of similarity detection technology of science fiction painting is highlighted, which can avoid malicious infringement by competitors. In essence, similarity detection technology of science fiction painting belongs to the field of image detection technology. Although image detection technology is widely used in biomedicine, communication, machine vision and other fields, there is still a large gap in similarity detection of science fiction painting.

Traditionally, image detection mainly includes extraction of target image and image similarity measurement. The essence of target image extraction is to locate and separate the object of interest from the image to be detected. It can suppress the influence brought by the content of the non-main target area, thereby improving the accuracy of image detection. In recent years, target image extraction technology based on machine learning [2, 29] has been favored by many researchers. Although it has broad development prospects, it cannot be realized without a huge training set and test set, and science fiction painting does not have this condition at present. However, the traditional template matching (TM) can extract the target image or the image with high similarity to the target image from the image to be detected without a huge training set and test set. TM is one of the classical image matching techniques in computer vision, and it is a pattern recognition method that can be easily combined with the new algorithm, which is widely used in target tracking, target recognition and target detection. There are two core parts in TM: objective function and search strategy. Template matching methods commonly use in existing studies evaluate the similarity between images by an exhaustive calculation (search strategy) of the normalized cross-correlation (NCC) values (similarity metric) of all elements in the source image. However, this exhaustive search is a computationally expensive operation and its application scenarios have significant limitations, especially in some real-time detection. To reduce the computational time of NCC, scholars have proposed several search strategies based on swarm intelligence optimization algorithms and its variants, such as material state evolution algorithm [7], locust swarm algorithm [13], internal feedback artificial bee colony algorithm [20], and hybrid Rao-nm algorithm [24]. Although these algorithms aim to reduce the computational effort of global optimal search, their matching accuracy and real-time performance remain low, and they cannot avoid the generation of suboptimal matching results. Besides, image similarity measurement is an important basis to judge whether the extracted target image is similar to the template image. For practical application scenarios, the selection of similarity measurement method has a direct impact on the validity and reliability of the final detection results. Common methods include image distance [3], singular value decomposition (SVD) [38], color histogram [35], SIFT algorithm [15], etc.

Sparrow search algorithm (SSA) is a new optimization algorithm constructed by Chinese scholar Xue J by modeling the predation and anti-predation behavior of sparrows. SSA is superior to GWO, PSO and GSA in terms of accuracy, convergence speed, stability and robustness [44]. Therefore, it has attracted the attention and research of many scholars in the past year, and has been successfully applied in the fields of hemispherical vortex

generator [40], gear fault diagnosis [9], microgrid energy management system [31], efficiency of solar photovoltaic energy system [10], steady-state visual evoked potential [4] and so on. However, SSA has the same problems as other intelligent optimization algorithms [32], such as premature convergence, and it also exposes three shortcomings : (1) the position of producers shows a gradual decrease as the iteration progresses; (2) it only focuses on the improvement of global search ability, and ignores the balance between local development ability and global search ability; (3) when the population size is relatively large or the sparrow population converges, the position of the scroungers tends to the origin. Faced with these problems, many scholars put forward their own improvement strategies, which are mainly divided into four aspects:

(1) Initialize the population. For the swarm intelligence optimization algorithm of population iteration, the diversity of initial population affects the search efficiency and global convergence of the algorithm to a certain extent. Like most intelligent optimization algorithms, SSA randomly generates the initial position of the sparrow population. The random generation method often leads to uneven distribution of the initial position of the sparrow, which increases the number of invalid searches of the algorithm. Improving the initial population is one of the common ways to improve algorithm performance, so there are many studies in this area. Xiong Q et al. [43] initializes the population by fractional chaotic mapping, so that the initial sparrow individuals are distributed as evenly as possible. Wu C et al. [41] adopts greedy algorithm to replace the random generation of the population in the original SSA, which not only maintains the diversity of the population, but also improves the efficiency of the algorithm. Liu G et al. [22] uses cubic mapping chaos sequence to generate population of CASSA, and the ergodicity and initial sensitivity of chaotic mapping improve the diversity of the population. Chaotic mapping is ergodic, which can effectively improve the global optimization ability of the algorithm. Therefore, Wang P et al. [39] proposes Bernoulli chaotic mapping to generate the initial position of sparrows.
(2) Location update mechanism. In SSA, the search is carried out through the coordination of producers, scroungers and scouts, so the location update mechanism plays a leading role in the process of SSA optimization. However, the location updating mechanism of SSA itself has some drawbacks. For example, the location of producers gradually decreases with the iteration, and SSA has problems such as premature convergence and low solution accuracy in the late searching period. Therefore, some scholars put forward many strategies to modify the location update mechanism. Song C et al. [34] introduces the global optimal solution and dynamic weighting factor of the previous generation in the location update phase of producer, and improves the position update mechanism of scout by combining the optimal position and the worst position. Jiang F et al. [14] uses Levy flight to update the positions of producers and scouts. Yan S et al. [45] adopts an improved iterative local search strategy in the position update mechanism of scrounger, and introduces a variable spiral factor to make the scroungers search more careful and flexible. Chen G et al. [6] introduces the alternative Gaussian Mutation to improve the position updating ability of producers, and adds a uniform mutation operator to the position updating mechanism of scouts to avoid excessive aggregation or divergence of populations.
(3) Adaptive factor. A successful algorithm not only ensures the convergence of the algorithm, but also considers the balance between the global search ability and local development ability of the algorithm. Therefore, introducing adaptive factors into SSA is the most common solution strategy. According to current research results, there are

generally two ways to introduce adaptive factors into SSA :(a) introducing adaptive factors in the position update stage. Liang Q et al. [21], Ouyang C et al. [30] and Tian Z et al. [36] introduce inertial weights into the position updating mechanism of producer for adaptive adjustment, while Zhu Y et al. [54] adds adaptive learning factors into all position updating mechanisms to improve the existing problems of SSA. (b) A nonlinear decreasing strategy is proposed for dynamic control of the number of scouts. Wu Y et al. [42] and Zhang C et al. [49] balance global search capability and local development capability by dynamically adjusting the number of scouts.

(4) Fusion of other algorithms. Fusion with other algorithms is now a new breakthrough about algorithm improvement. Although different algorithms may get different results in dealing with the same optimization problem, it is also an effective way to directly improve SSA by integrating the prominent optimization mechanism of other intelligent optimization algorithms on the basis of SSA. Zhou S et al. [53] introduces crossover and mutation operations of GA, so that the improved SSA has a higher convergence speed and greater enhancement effect than the original SSA. Kathiroli P et al. [18] adopts the hybrid sparrow search algorithm of differential evolution, which gives full play to the characteristics of DE and SSA, and also enhances the potential search diversity of SSA. Zhang J et al. [50] adopts the sine and cosine algorithm as a hybrid algorithm to help SSA jump out of local optimum and introduces a new structure of division of labor to rapidly converge to the global optimum solution. Yang L et al. [46] combines SSA with PSO, and verifies that the optimization performance of the hybrid algorithm (SSA-PSO) is better than that of the single algorithm.

Although these strategies can effectively improve the optimization capability of SSA to a certain extent and accelerate the matching speed, the swarm intelligence optimization algorithm itself is probabilistic, so it may not be able to guarantee the accuracy and real-time performance of matching. Considering that there is a template matching method with Gaussian pyramid hierarchical matching as the search strategy and NCC as the objective function, it can obtain the highest accuracy of matching results and reduce unnecessary operations. Although the computation cost is reduced compared with NCC algorithm, the time-consuming aspect can still be improved. SSA has poor accuracy and stability in the matching process, but the convergence speed is fast. Practical applications have high requirements for both accuracy and real-time similarity detection of science fiction paintings, and the existing similarity work only satisfies one of them. Therefore, unlike similar existing works, a template matching method (MISSA-GP-TM) based on multi-strategy improved sparrow search algorithm (MISSA) and Gaussian pyramid (GP) is proposed in this paper by combining the shortcomings and advantages of Gaussian pyramid and SSA. The method utilizes the hierarchical matching of Gaussian pyramid matching algorithm to improve the matching accuracy, and the search strategy based on MISSA to further reduce the matching time. According to the relevant characteristics of the two algorithms, combining them can achieve complementary effects and can simultaneously provide accuracy and real-time performance. In terms of algorithm improvement, MISSA adopts a hybrid search strategy based on step function in the position update stage of producer, dynamically controls safety threshold at multiple stages, and proposes a food search strategy based on Logistic model in the position update stage of scrounger. In terms of performance verification of MISSA, all tests are implemented on the CEC2017 benchmark function, and the experimental results are analyzed by Wilcoxon signed rank test [11] and Freidman test [8]. The rationality and effectiveness of the three improved strategies to improve SSA are verified by ablation experiment, and MISSA is compared with four classical algorithms and

three improved SSA. The final comprehensive ranking results show that optimization ability of MISSA is better than that of peer algorithms. Gaussian pyramid adopts a coarse-to-fine matching strategy, and searches for the best matching point by taking the rough matching from the previous layer as the starting point. But since the top layer has no initial target location from the previous layer, it must perform a global search pixel by pixel. Therefore, MISSA with strong global optimization ability is selected to replace the ergodic search on the top subgraph of Gaussian pyramid to save the matching time and provide rough initial matching position for the next layer. In the experiment of similarity detection of science fiction painting, MISSA-GP-TM algorithm is used in the extraction of target image of science fiction painting, and perceptual hash (pHash) [48] is used as similarity measurement index to calculate the similarity of matching results. The comparison results of detection show that MISSA-GP-TM performs the best in terms of running time, similarity and robustness under different sizes.

In summary, the main contributions of this paper are as follows:

- An improved sparrow search algorithm based on multiple strategies is proposed. A hybrid search strategy based on step function is adopted in the position update stage of producer, safety threshold is dynamically controlled at multiple stages, and a food search strategy based on Logistic model is proposed in the position update stage of scrounger.
- Ablation experiment is used to verify whether each strategy could improve the algorithm.
- Compared with four classical algorithms and three improved algorithms, strong optimization ability of MISSA is verified.
- A target image extraction method based on multi-strategy improved sparrow search algorithm and Gaussian pyramid is proposed, and perceptual hashing is used to calculate the similarity of matching results of science fiction painting. Experimental results show that MISSA-GP-TM can obtain stable and reliable detection results.

The rest of this paper is organized as follows. Section 2 mainly expounds the relevant theoretical background, and introduces the multi-strategy improved sparrow search algorithm and the similarity detection method of science fiction painting in detail. Section 3 verifies the performance of MISSA through ablation experiments, comparison with peer algorithms, and analysis of time complexity and diversity of algorithm. Section 4 is mainly the simulation experiment of the similarity detection of science fiction painting. Finally, Section 5 is some summary of the full text work.

2 Theory

2.1 Related theoretical background

2.1.1 Template matching based on Gaussian pyramid

In the image pyramid, the resolution of sub-images arranged in pyramid shape decreases from bottom to top. Its bottom layer is a high-resolution representation of the original image, and the top layer is a low-resolution representation. Therefore, image pyramid can describe the image information in a multi-scale way and can be used to construct features or solve the problem of image analysis scale. Gaussian pyramid is a kind of image pyramid widely used in the field of image processing. It is a kind of image structure interpreted

by multi-resolution, and n layers of sub-images with different resolutions are generated by multi-scale pixel sampling of the original image. The core process of constructing gaussian pyramid is as follows: Gaussian image of n+1 layer can be obtained by gaussian smoothing and down-sampling for the n layer of Gaussian pyramid. The Gaussian pyramid contains a series of low-pass filters, whose frequency increases gradually by factor 2 from the upper layer to the next layer, so it has the advantage of spanning a large frequency range and can better describe the image at multiple scales. Figure 1 shows the hierarchical diagram of the Gaussian pyramid. If the original image is large, the time of calculation for traversing the entire original image is generally very long when we perform traditional template matching. Therefore, the template matching algorithm based on Gaussian pyramid is often used for hierarchical matching to solve this problem. The general process is as follows:

(1) The number of layers and window range of pyramid is set, and the measure of similarity during matching is the normalized correlation coefficient (NCC).
(2) The k-layer pyramid image is created for the source image to be processed and template image, which mainly involves down-sampling (divided by 2) and Gaussian smoothing filter processing.
(3) Matching starts from the top of the pyramid, and the best matching position obtained is passed to the lower layer in turn (multiplied by 2). It is worth noting that the top layer of the pyramid requires a complete ergodic matching. According to the position passed by the previous layer as the search starting point, pixel-by-pixel matching is performed within the set window range, and the process is repeated until the bottom layer.

2.1.2 Sparrow search algorithm

The sparrow search algorithm is inspired by the division and collaboration of sparrows in social life. According to the division of labor in the foraging and anti-predation process of

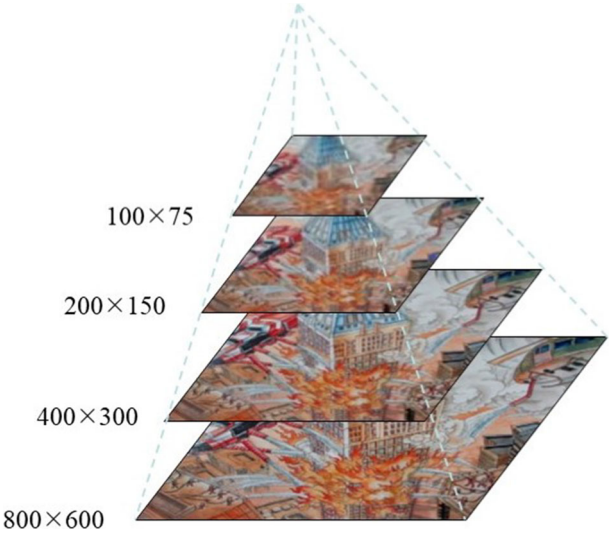

Fig. 1 Hierarchical diagram of the Gauss pyramid

different sparrows, they are specifically divided into producers, scroungers and scouts. During the process of sparrow foraging, the producer conducts a large-scale search to determine the foraging area and direction of the entire population, and the scrounger searches for food according to the information provided by the producer. As long as the energy reserves are high or a better food source is found, any sparrow can become a producer, but the ratio of producer to scrounger remains the same in the entire population. In the anti-predation process, it issues an alarm in time and decides whether to evacuate the dangerous area when the scout is aware of the danger.

For producers:

$$x_i^{t+1} = \begin{cases} x_i^t.exp(\frac{-i}{\alpha.T_{max}}), R_2 < S \\ x_i^t + Q.L, R_2 \geq S \end{cases} \tag{1}$$

where x_i^t is the position of the i-th producer at the t-th iteration. $S(S \in [0.5, 1])$ is the safety threshold. $R_2(R_2 \in [0, 1])$ is the warning value. $\alpha(\alpha \in (0, 1))$ is is a random number. T_{max} is the maximum number of iterations. L is a d-dimensional row vector with all elements 1. Q is a random number that obeys a normal distribution. When $R_2 < S$, there is no potential danger in the foraging environment and producers can conduct a full range of searches within the foraging area. When $R_2 \geq S$, some producers perceive the existence of danger and adjust the search route, and all individuals leave their current positions to avoid being hunted by natural enemies.

For scroungers:

$$x_i^{t+1} = \begin{cases} Q.exp(\frac{x_{worst}^t - x_i^t}{i^2}), i > \frac{P}{2} \\ x_p^{t+1} + |x_i^t - x_p^{t+1}|.A^+.L, otherwise \end{cases} \tag{2}$$

where P is the population size of sparrows. x_{worst}^t is the current worst foraging position. x_p^{t+1} is the position of the producer with the optimal fitness value at the $t+1$ iteration. A represents a column vector of the same dimension as the sparrow individual, the internal elements are composed of 1 and -1, and $A^+ = A^T(AA^T)^{-1}$. When $i \leq \frac{P}{2}$, the scrounger actively follows the producer to search around the best foraging location. When $i > \frac{P}{2}$,the scrounger flies to other places in search of food to escape his hunger.

For scouts:

$$x_i^{t+1} = \begin{cases} x_{best}^t + \beta.|x_i^t - x_{best}^t|, f_i > f_g \\ x_i^t + K.(\frac{|x_i^t - x_{worst}^t|}{(f_i - f_w) + \epsilon}), f_i = f_g \end{cases} \tag{3}$$

where f_i, f_g are the fitness value of the current scout and the global optimal fitness value respectively, and f_w is the worst fitness value. x_{best}^t is the current global optimal position. β represents a step-length control parameter that obeys the standard normal distribution. ϵ is a constant used to prevent the denominator from being zero. $K(K \in [-1, 1])$ is a random number. When $f_i > f_g$, the scout at the edge of the population perceives the approach of the predator, and then moves toward the food-filled area. When $f_i = f_g$, the scout in the center of the population moves to other individuals for protection to reduce the risk of predation.

2.2 Improved sparrow search algorithm based on multiple strategies (MISSA)

2.2.1 Hybrid search strategy based on step function

In SSA, the producer is the guide of the iterative search of the algorithm, responsible for searching a large area and providing the approximate location of the food for the entire population, but the original search strategy of the producer fails to achieve this goal. It can be seen from (1) that the position of the producer shows a gradual decrease as the

iteration progresses when when $R_2 < S$, which means that the foraging area that can be explored by the entire population only gets smaller and smaller, and the probability of getting a sub-optimal solution also increases. At present, various types of search strategies have appeared in swarm intelligence optimization algorithms, which to a large extent determine the performance of the algorithm. Common search strategies are:

$$x_i^{t+1} = x_i^t + k_1.rand().(x_{r_1}^t - x_i^t) + k_2.rand().(x_{r_2}^t - x_i^t) \tag{4}$$

$$x_i^{t+1} = x_i^t + S.(r_2.x_{best}^t - r_3.x_i^t) \tag{5}$$

$$x_i^{t+1} = |x_{best}^t - x_i^t|.e^{bl}.cos(2\pi l) + x_{best}^t \tag{6}$$

$$x_i^{t+1} = x_i^t + \varphi_i.(x_i^t - x_k^t) \tag{7}$$

$$x_i^{t+1} = x_i^t + rand().fl_i^t.(x_{best}^t - x_i^t) \tag{8}$$

$$x_i^{t+1} = x_i^t + LF.(x_{r_1}^t - x_i^t) \tag{9}$$

Equation (4) is the position updating strategy of hen [25], (5) is the somersault foraging strategy [51], (6) is the spiral position updating strategy [26], (7) is the position updating strategy of lead bee [16], (8) is the position updating strategy of crow [37] and (9) is the nesting stage (nest) [28]. Among them, (4), (7) and (9) improve the global search ability of the algorithm by communicating with randomly selected individuals to generate candidate solutions, but the convergence speed is slow. While (5), (6) and (8) can enhance the local development ability of the algorithm by communicating with the optimal individual to generate candidate solutions, but may accelerate the convergence to suboptimal solutions. For swarm intelligence optimization algorithm, global search ability and local development ability both play an important role in the process of optimization, and they are indispensable. Although they have always been the focus of research of scholars, the traditional single search strategy is difficult to give consideration to both the global search ability and local development ability of the algorithm. Therefore, by analyzing the above strategies and combining their characteristics and shortcomings of producer in SSA, this paper proposes a hybrid search strategy based on step function in the position update stage of producer, and its expression is shown in (10).

$$x_i^{t+1} = x_i^t + exp(\frac{-i}{\alpha.T_{max}}).(k_1.(\varepsilon(p).x_{rand}^t + (1 - \varepsilon(p)).x_{best}^t) - k_2.x_i^t),\ R_2 < S \tag{10}$$

Where x_{rand}^t is a randomly selected sparrow individual, x_{best}^t is the sparrow with the best overall position, k_1 and k_2 are random numbers in (0, 1), $\varepsilon(p)$ is the redefined step function, as in (11).

$$\varepsilon(p) = \begin{cases} 1, & p \geq p_1 \\ 0, & p < p_1 \end{cases} \tag{11}$$

It can be seen from (10) that the hybrid search strategy based on step function combines the current sparrow individual, randomly selected sparrow individual and globally optimal sparrow individual to update their position. The specific implementation process is as follows:

when $p \geq 0.5$, (10) is simplified to:

$$x_i^{t+1} = x_i^t + exp(\frac{-i}{\alpha.T_{max}}).(k_1.x_{rand}^t - k_2.x_i^t) \tag{12}$$

when $p < 0.5$, (10) is simplified to:

$$x_i^{t+1} = x_i^t + exp(\frac{-i}{\alpha.T_{max}}).(k_1.x_{best}^t - k_2.x_i^t) \tag{13}$$

In (12), the new search strategy combines the current individual and the randomly selected individual, which can ensure the diversity of the search position of producer and avoid premature convergence of the algorithm to the suboptimal solution in the iterative process. In (13), the new search strategy combines the current individual and the globally optimal individual, which can directly guide the population to move closer to the optimal position and carry out local development. From the above analysis, it can be seen that the hybrid search strategy based on step function is to combine current individuals randomly with randomly selected individuals and globally optimal individuals through step function, which makes up for the deficiency of single strategy. This can not only give full play to their respective advantages, but also better balance the global search capability and local development capability of SSA in the case of enriching the optimal positions of producers.

2.2.2 Multi-stage dynamic control factors

As soon as the sparrow sees a potential danger around them, they chirp as an alarm signal. When R_2(Alarm signal)$< S$(Safety threshold), it means that the danger signal of the foraging area is removed, and the producer can continue to carry out large-scale search in other areas, which represents the global search ability of the algorithm. When $R_2 \geq S$, it means that the danger is approaching the sparrow population. The producer sends escape signals to other populations and guides them to escape to safe areas, which represents the local development ability of the algorithm.

In standard SSA, the safety threshold is usually a fixed parameter, which make the local development ability of the algorithm weak, resulting in low convergence accuracy in the later stage, and it is easy to converge to a suboptimal solution. In order to solve this problem, this paper proposes a multi-stage strategy to dynamically control the safety threshold, so that the producer can realize the global and local alternate search in the process of optimization, and balance the global search ability and local development ability of the algorithm.

Assuming that the total number of iterations of the algorithm is T,the entire iteration process is divided into m segments, the iteration number of each process is set to T_1, T_2, ..., T_m, and satisfies $T_1 + T_2 + ... + T_m = T$ [33]. In each iteration process, the population can adopt different safety thresholds. The safety threshold of multi-stage dynamic control is defined as (14).

$$S = f(lb_i, ub_i, T_i), i \in m \tag{14}$$

where lb_i and ub_i respectively represent the lower and upper bounds of the control factor, $f(.)$ is the defined linear or non-linear function, T_i represents the number of iterations in the i-th segment. Therefore, this paper designs a three-stage dynamic control safety threshold, as shown in (15).

$$S = \begin{cases} ub, t \leq T_1 \\ (ub - lb).[sin(\frac{\pi}{2}.(1 - \frac{t-T_1}{T_2-T_1})) + \frac{lb}{ub-lb}], T_1 < t < T_2 \\ lb, T_2 \leq t \leq T_{max} \end{cases} \tag{15}$$

Where $t \leq T_1$ and $T_2 \leq t \leq T_{max}$, the safety threshold (S) is the upper and lower bounds of the control factor respectively. When $T_1 < t < T_2$, the safety threshold (S) decreases nonlinearly from ub to lb. We can dynamically control the safety threshold at multiple stages. In the update position of producer in the early stage of algorithm evolution, the safety threshold remains at ub for a long time, which means that the producer focuses on global search. The producer explores the foraging area in a large range and guides the population to converge near the optimal location. As the iteration goes on, the safety threshold begins to nonlinear

decrease, and the global and local alternate search is realized to avoid the sudden stagnation of the population. At the late stage of evolution, the safety threshold is lb for a long time, which means that the producer tends to focus on local development. The producer performs local development near the optimal location to approximate the optimal solution of the algorithm. Therefore, the new position of the producer in MISSA is updated as shown in (16).

$$x_i^{t+1} = \begin{cases} x_i^t + exp(\frac{-i}{\alpha.T_{max}}).(k_1.(\varepsilon(p).x_{rand}^t + (1-\varepsilon(p)).x_{best}^t) - k_2.x_i^t), R_2 < S \\ x_i^t + Q.L, R_2 \geq S \end{cases} \tag{16}$$

2.2.3 Food search strategy based on Logistic model

In (2), when $i > \frac{P}{2}$, the scrounger who fails to compete for food combines with exp function characteristics to get rid of the current poor foraging position and actively flies to other foraging areas. However, we found that if the sparrow population converges or the population size is relatively large, its value gradually approaches the origin, which means that the scrounger cannot seek a better foraging position, and they fall into suboptimal solution early due to ignoring the search blind spot and insufficient search range in the search process. In the exploration stage of whale optimization algorithm, whales update their own positions through location of each other, which forces whales to stay away from the location of prey and enables the algorithm to have certain global optimization capability. The mathematical model is shown in (17). The control parameter (a) decreases linearly with the iteration, which means that the global optimization ability also decreases linearly. However, this linear decreasing factor is difficult to be applied to the optimization of high-dimensional complex functions.

$$x_i^{t+1} = x_{rand}^t - (2.r_1 - 1).a.|C.x_{rand}^t - x_i^t| \tag{17}$$

$$a = 2 - 2.\frac{t}{T_{max}} \tag{18}$$

Therefore, this paper combines the advantages and disadvantages of WOA in the prey search stage and the adaptive factor based on the Logistic model in the literature [5], and proposes a food search strategy based on the Logistic model in the position update stage of scrounger. The mathematical model is shown in (19).

$$x_i^{t+1} = x_{rand}^t - G.(\frac{1}{1+e^{at+b}} + w).|x_{rand}^t - x_i^t| \tag{19}$$

Where a and b represent expansion and translation factors respectively, G represents amplitude gain, and $w(w \in [0, 1))$ can dynamically adjust the upper and lower bounds of parameters. In the iterative process of the algorithm, the location of an individual sparrow is randomly selected as the target location for exploration and development, which is beneficial to enhance the global optimization ability of the algorithm and avoids stagnation of the algorithm. The Logistic model is a nonlinear decreasing function, which can coordinate the global search and local development of the algorithm, so that the algorithm slows down the convergence speed in the position update stage of scrounger in the early iteration to perform a full global search, and focus on the development around the target position and speed up the convergence in the later iteration. Therefore, the new position of the scrounger in MISSA is updated as shown in (20).

$$x_i^{t+1} = \begin{cases} x_{rand}^t - G.(\frac{1}{1+e^{at+b}} + w).|x_{rand}^t - x_i^t|, i > \frac{P}{2} \\ x_p^{t+1} + |x_i^t - x_p^{t+1}|.A^+.L, otherwise \end{cases} \tag{20}$$

2.2.4 Flow chart of MISSA algorithm

In summary, the overall flowchart of the proposed MISSA is shown in Fig. 2.

2.2.5 Time complexity analysis of MISSA

The improvement strategy adopted by MISSA is mainly in the position update stage of producer and scrounger, and the other stages are the same as traditional SSA. Therefore, we mainly conduct time complexity analysis in the position update stage of producer and scrounger.

In SSA, the population size is P, the optimized spatial dimension is d, and the time to solve the target fitness function is $f(d)$. The number of producers is $pNum$, the time of position update in each dimension according to (1) is t_1, and the generation time of random numbers Q and α is η_1, so the time complexity of the location update stage of producer in SSA is $T_1 = O(pNum.((t_1 + \eta_1).d + f(d)))$. The number of scroungers is $(p - pNum)$, the time of position update in each dimension according to (2) is t_2, and the generation time of random number Q and row vector A is η_2, so the time complexity of the location update stage of producer in SSA is $T_2 = O((P - pNum).((t_2 + \eta_2).d + f(d)))$. The total time is $T = T_1 + T_2 = O(d + f(d))$.

Among the producer of MISSA, the time of position update in each dimension according to (16) is t_3, the time of multi-stage dynamic control safety threshold is η_3, the generation time of random numbers Q and α is η_4, so the time complexity of the improved producer is $T_3 = O(pNum.((t_3 + \eta_4).d + f(d)) + \eta_3)$. In the scrounger, the time for location update for each dimension according to (20) is t_4, and the generation time of random number

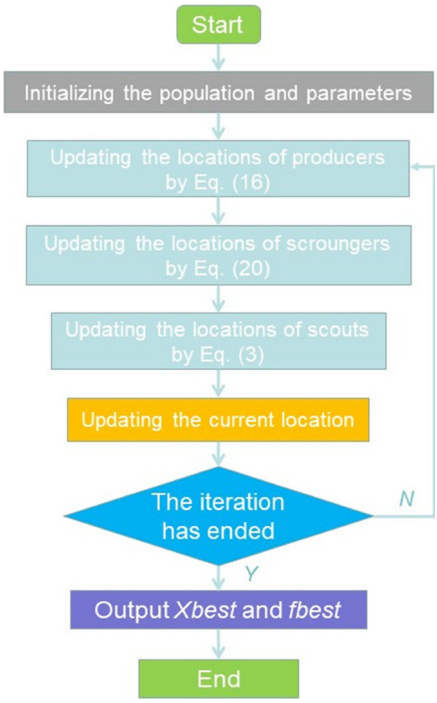

Fig. 2 Flowchart of the proposed MISSA

Q and row vector A is η_5, so the time complexity of the improved scrounger is $T_4 = O((P - pNum).((t_4 + \eta_5).d + f(d)))$. The total time after improvement is $T' = T_3 + T_4 = O(d + f(d))$. In summary, comparing MISSA and SSA, the time complexity of the algorithm is the same, which means that the improvement strategy proposed in this paper for SSA does not increase the time complexity of the algorithm.

2.3 Similarity detection method of science fiction painting

Similar to the traditional image detection methods, the similarity detection of science fiction painting mainly includes two aspects: extraction of target image and image similarity measurement. In object image extraction, a template matching method (MISSA-GP-TM) based on MISSA and GP is proposed. GP can reduce the time of image matching on the basis of effectively retaining most of the information in the image through the idea of hierarchical matching. It takes the matching point of the upper layer as the center point of the lower layer image matching, but the top layer of the GP needs to be completely ergodic matching. In general, when the NCC reaches its maximum value, the two images are in the correct matching position. From the point of view of optimization, the ergodic matching of top layer can be regarded as a single objective optimization problem. Therefore, we choose MISSA with strong global optimization ability to replace the traditional ergodic matching at the top of the pyramid, and use MISSA to obtain the best initial matching center to maximize NCC. This not only makes up for low accuracy and stability of MISSA in template matching, but also further speeds up matching speed of GP. Firstly, a k-layer pyramid image is created for the source image to be matched and the template image. Then, MISSA is used to perform rough matching in the top subgraph of the source image to be matched to obtain the coordinates of the initial matching target. Finally, the location transferred from the layer above each layer is the starting point of search, and pixel by pixel matching is carried out within the set window range. The specific implementation steps of MISSA-GP-TM algorithm are as follows:

Step1. Create k-layer pyramid image for the image to be matched and template image respectively;

Step2. In the k-layer subgraph, MISSA is used for rough matching to obtain the coordinates of the initial matching target. The optimization process of MISSA is as follows:

- (a) Parameter initialization: population size (P), maximum iteration T_{max} and dim, population initialization, NCC as fitness function.
- (b) The global optimal position is updated through the position update of (16), (20) and (3).
- (c) If the iteration termination condition is met (or the best matching position is found), the optimal solution is output; otherwise, step (b) is continued.

Step3. Set the window range to $m \times m$, and the optimal solution is taken as the initial matching center to transfer to k-1 layer in turn, and the subgraph to be matched and the template subgraph of the same layer are matched pixel by pixel within the scope of the window to obtain the best matching position.

Step4. If K=0, the algorithm ends and the final matching region is output. Otherwise, go to Step3.

Perceptual hashing algorithm has been widely used in image retrieval, image quality assessment, detection of image replication and other fields. It has the advantages of simplicity, speed and good robustness. As the detection object is a science fiction painting, its deformation degree is not very large and rotation rarely occurs. Therefore, in terms of image similarity measurement, we choose perceptual hash (pHash) as the measurement index between the extracted target image and template image, which is reasonable and effective. The pHash mainly performs DCT transformation on the image, obtains the mean value of DCT coefficients, and realizes image similarity calculation based on the characteristics of its transform domain. The specific implementation process is as follows:

(a) Reduce the size of the image;
(b) Transform the image into grayscale image;
(c) DCT coefficient matrix of 32×32 is obtained by discrete cosine transform of gray image;
(d) The DCT coefficient matrix is reduced to preserve only the 8×8 matrix in the upper left corner;
(e) Calculate the mean value of the reduced DCT coefficient matrix;
(f) Calculate the hash value and compare the elements in the 8×8 DCT matrix with the mean value. If the value is greater than the mean value, it is recorded as 1. Otherwise, it is 0. Finally, the recorded data are combined together to obtain the image fingerprint.
(g) Calculate the Hamming distance between the images to be compared, so as to judge the similarity between them.

3 Numerical simulation

3.1 Simulation environment

In order to ensure the fairness and objectivity of the comparison results, the same parameter settings are adopted for all the algorithms, with the population size being 100, the maximum evaluation times (FEs) being 3×10^5, and the optimization tests are conducted on the CEC2017 benchmark function, and the dimension in the benchmark function is set as 30. CEC 2017 consists of four different groups of functions: unimodal functions (F1-F3), simple multi-modal functions (F4-F10), hybrid functions (F11-F20), and composition functions (F21-F30). This diversity of functions is suitable to compare the proposed MISSA with the compared algorithms in terms of its ability to escape from local optima, convergence behavior, local search, and global search [47]. Each algorithm is run independently for 30 times, the average value (AVG) and standard deviation (STD) of each algorithm are recorded, and the best value obtained in the same benchmark function is marked with the bold term. Wilcoxon signed-rank test [11] and Freidman test [8] are used to evaluate whether MISSA has significant performance differences with other algorithms at the significance level of $p = 5\%$. Wilcoxon signed-rank test compares the performance of the algorithms in each benchmark function, Freidman test calculates and sorts the average performance of the algorithm in the benchmark function [52]. Mean represents the average of the overall ranking, and Rank represents the final ranking of the algorithm. $+$ indicates that the performance of the specified algorithm is better than that of other algorithms. $-$ indicates that the performance of the specified algorithm is worse than that of other algorithms. $=$ indicates that the performance of the specified algorithm is close to that of other algorithms. All tests are performed on a computer with AMD Ryzen 5 4600H with Radeon Graphics CPU, 16 G RAM (3200

MHz), and Windows 11 operating system, and the program language is implemented on MATLAB R2018a.

3.2 Sensitivity analysis on controlling parameters

The standard sparrow search algorithm is very sensitive to the choice of the safety threshold S. Therefore, the proposed MISSA algorithm uses the multi-stage dynamic control factors (15) to make this parameter adaptive. The whole iterative process is divided into early (0 - T_1), middle (T_1 - T_2) and late (T_2 - T_{max}) stages by T_1 and T_2. Since the maximum number of iterations = the maximum number of evaluations / number of populations involved in the evolutionary calculation, where the maximum number of evaluations is 3×10^5, and the actual number of populations involved in the calculation in the SSA is 150, the maximum number of iterations (T_{max}) here is 2000. In order that the producers can better realize the alternating global and local search in the process of finding the best, we set the time of the middle period to double the time of the first period and the second period, so $T_1 = 500$, $T_2 = 1500$ in the (15). It is worth noting that the equation depends mainly on the two parameters ub and lb, since they represent the upper and lower limits of the variation of the safety threshold S. In this section, the parameters ub and lb are investigated in order to find their optimal settings. The producer of MISSA requires the realization of alternating global and local search throughout the optimization process to avoid population stagnation. While in the early evolutionary stage of the algorithm, the more focus on global search in the case of achieving alternating global and local search at the same time is beneficial to increase the diversity of the population. In the late evolutionary stage of the algorithm, it tends to focus on local exploitation, which is beneficial to accelerate the population convergence. We therefore choose some of these values in a uniformly distributed manner in the range 0 to 1: 0.2, 0.4, 0.6, 0.8, where the parameters ub are set to 0.6 and 0.8, and the parameters lb are set to 0.2 and 0.4, and keep the other parameters fixed. By combining them two by two, four different sets of upper and lower bounds are generated. The four sets of data in Table 1 show the effect of different parameter (ub and lb) settings on MISSA. From the results of Wilcoxon signed-rank and Freidman tests in Table 1, it is clear that MISSA performs best when $ub = 0.8$ and $lb = 0.2$. Also, the p-values obtained from the Wilcoxon signed-rank test in Table 2 show that MISSA ($ub = 0.8$, $lb = 0.2$) has a more significant boost on most of the benchmark functions compared to the other three sets of parameter settings. Therefore, $ub = 0.8$ and $lb = 0.2$ is the best choice for MISSA.

In addition, setting p_1 to 0.5 in the hybrid search strategy based on the step function can combine the current individual with random individuals and the global optimal individual with equal probability, which can better balance the global search ability and local exploitation ability and make up for the shortage of a single strategy. In the food search strategy based on the Logistic model, the Logistic model is obtained by scaling and translating the Sigmoid function, as well as considering the maximum number of iterations to be 2000, so a is set to 1/100, and b is set to -10, making the range of variables adjusted to [0,2000] as to meet the practical application here. To ensure the diversity of the population in the nonlinear decreasing change, we set G as a random number and w as 0 in the Logistic model.

Table 1 Comparison of optimization results of MISSA under different parameter settings

Fun	Item	SSA	MISSA (ub=0.6,lb=0.2)	MISSA (ub=0.6,lb=0.4)	MISSA (ub=0.8,lb=0.2)	MISSA (ub=0.8,lb=0.4)
F1	AVG	$6.211E+03$	$3.736E+03$	$4.565E+03$	$4.126E+03$	$\mathbf{2.749E+03}$
	STD	$5.538E+03$	$4.634E+03$	$4.823E+03$	$4.191E+03$	$\mathbf{4.036E+03}$
F3	AVG	$3.059E+03$	$4.492E+02$	$4.093E+02$	$4.618E+02$	$\mathbf{4.039E+02}$
	STD	$1.385E+03$	$\mathbf{1.169E+02}$	$9.658E+01$	$1.317E+02$	$1.558E+02$
F4	AVG	$4.708E+02$	$4.662E+02$	$4.732E+02$	$\mathbf{4.464E+02}$	$4.752E+02$
	STD	$2.845E+01$	$3.462E+01$	$2.196E+01$	$3.161E+01$	$\mathbf{1.830E+01}$
F5	AVG	$7.189E+02$	$6.895E+02$	$\mathbf{6.809E+02}$	$6.880E+02$	$6.832E+02$
	STD	$3.381E+01$	$4.491E+01$	$\mathbf{2.724E+01}$	$3.051E+01$	$3.865E+01$
F6	AVG	$6.414E+02$	$6.317E+02$	$6.330E+02$	$\mathbf{6.292E+02}$	$6.390E+02$
	STD	$\mathbf{8.634E+00}$	$1.131E+01$	$1.184E+01$	$1.149E+01$	$1.088E+01$
F7	AVG	$1.152E+03$	$1.017E+03$	$\mathbf{9.898E+02}$	$1.017E+03$	$1.037E+03$
	STD	$1.087E+02$	$8.975E+01$	$\mathbf{7.621E+01}$	$7.972E+01$	$1.042E+02$
F8	AVG	$9.554E+02$	$\mathbf{9.359E+02}$	$9.431E+02$	$9.420E+02$	$9.388E+02$
	STD	$3.057E+01$	$2.832E+01$	$2.310E+01$	$\mathbf{1.862E+01}$	$2.568E+01$
F9	AVG	$5.201E+03$	$9.359E+02$	$9.431E+02$	$3.528E+03$	$\mathbf{9.388E+02}$
	STD	$\mathbf{5.874E+02}$	$8.219E+02$	$1.084E+03$	$7.408E+02$	$8.464E+02$
F10	AVG	$5.155E+03$	$4.187E+03$	$3.474E+03$	$4.964E+03$	$\mathbf{3.391E+03}$
	STD	$\mathbf{5.204E+02}$	$9.045E+02$	$6.616E+02$	$6.188E+02$	$7.387E+02$
F11	AVG	$1.355E+03$	$1.233E+03$	$\mathbf{1.228E+03}$	$1.245E+03$	$1.279E+03$
	STD	$7.106E+01$	$\mathbf{4.745E+01}$	$6.249E+01$	$6.596E+01$	$9.107E+01$
F12	AVG	$1.146E+05$	$7.775E+04$	$7.306E+04$	$\mathbf{6.527E+04}$	$7.578E+04$
	STD	$5.794E+04$	$5.158E+04$	$4.082E+04$	$\mathbf{3.313E+04}$	$4.398E+04$
F13	AVG	$3.020E+04$	$\mathbf{1.465E+04}$	$1.813E+04$	$1.503E+04$	$1.529E+04$
	STD	$2.601E+04$	$1.644E+04$	$1.932E+04$	$\mathbf{1.614E+04}$	$1.799E+04$
F14	AVG	$1.323E+04$	$8.765E+03$	$1.017E+04$	$\mathbf{8.056E+03}$	$8.986E+03$
	STD	$6.732E+03$	$4.801E+03$	$7.363E+03$	$\mathbf{4.037E+03}$	$5.648E+03$
F15	AVG	$1.181E+04$	$\mathbf{8.889E+03}$	$1.645E+04$	$1.140E+04$	$9.443E+03$
	STD	$1.175E+04$	$\mathbf{7.587E+03}$	$1.490E+04$	$1.380E+04$	$9.899E+03$
F16	AVG	$2.879E+03$	$2.766E+03$	$2.775E+03$	$2.792E+03$	$\mathbf{2.703E+03}$
	STD	$2.748E+02$	$2.832E+02$	$3.158E+02$	$\mathbf{2.076E+02}$	$3.425E+02$
F17	AVG	$2.537E+03$	$2.378E+03$	$2.350E+03$	$\mathbf{2.286E+03}$	$2.322E+03$
	STD	$\mathbf{1.779E+02}$	$2.393E+02$	$2.347E+02$	$1.784E+02$	$1.964E+02$
F18	AVG	$2.940E+05$	$1.686E+05$	$1.635E+05$	$2.001E+05$	$\mathbf{1.550E+05}$
	STD	$2.457E+05$	$\mathbf{1.330E+05}$	$1.818E+05$	$1.389E+05$	$1.501E+05$
F19	AVG	$2.421E+04$	$1.205E+04$	$1.047E+04$	$\mathbf{6.410E+03}$	$1.104E+04$
	Std	$2.282E+04$	$1.209E+04$	$\mathbf{7.487E+03}$	$8.787E+03$	$1.105E+04$
F20	AVG	$2.633E+03$	$2.565E+03$	$2.594E+03$	$\mathbf{2.253E+03}$	$2.569E+03$
	STD	$\mathbf{1.975E+02}$	$2.075E+02$	$2.518E+02$	$1.977E+02$	$2.465E+02$
F21	AVG	$2.518E+03$	$\mathbf{2.449E+03}$	$2.451E+03$	$2.453E+03$	$2.463E+03$
	STD	$5.873E+01$	$\mathbf{2.289E+01}$	$3.296E+01$	$2.635E+01$	$4.492E+01$
F22	AVG	$4.224E+03$	$4.741E+03$	$4.745E+03$	$\mathbf{3.136E+03}$	$3.632E+03$
	STD	$2.297E+03$	$2.552E+03$	$2.242E+03$	$\mathbf{1.724E+03}$	$2.089E+03$

Table 1 (continued)

Fun	Item	SSA	MISSA (ub=0.6,lb=0.2)	MISSA (ub=0.6,lb=0.4)	MISSA (ub=0.8,lb=0.2)	MISSA (ub=0.8,lb=0.4)
F23	AVG	$2.866E+03$	$2.865E+03$	$2.855E+03$	$\mathbf{2.822E+03}$	$2.846E+03$
	STD	$4.608E+01$	$6.854E+01$	$7.584E+01$	$\mathbf{4.474E+01}$	$6.630E+01$
F24	AVG	$3.077E+03$	$3.027E+03$	$\mathbf{3.002E+03}$	$3.011E+03$	$3.043E+03$
	STD	$8.673E+01$	$6.572E+01$	$5.159E+01$	$\mathbf{4.244E+01}$	$8.127E+01$
F25	AVG	$2.890E+03$	$2.893E+03$	$2.901E+03$	$\mathbf{2.888E+03}$	$2.891E+03$
	STD	$7.374E+00$	$1.393E+01$	$2.244E+01$	$8.184E+00$	$\mathbf{1.068E+01}$
F26	AVG	$5.803E+03$	$5.669E+03$	$5.834E+03$	$5.919E+03$	$\mathbf{5.319E+03}$
	STD	$\mathbf{9.018E+02}$	$9.168E+02$	$9.077E+02$	$9.675E+02$	$1.256E+03$
F27	AVG	$3.248E+03$	$3.245E+03$	$3.253E+03$	$\mathbf{3.245E+03}$	$3.248E+03$
	STD	$2.246E+01$	$2.343E+01$	$3.344E+01$	$\mathbf{1.873E+01}$	$4.274E+01$
F28	AVG	$3.183E+03$	$3.170E+03$	$\mathbf{3.125E+03}$	$3.135E+03$	$3.160E+03$
	STD	$5.519E+01$	$6.292E+01$	$\mathbf{5.255E+01}$	$5.983E+01$	$5.955E+01$
F29	AVG	$4.187E+03$	$\mathbf{3.944E+03}$	$4.007E+03$	$4.043E+03$	$4.002E+03$
	STD	$2.684E+02$	$\mathbf{2.278E+02}$	$2.565E+02$	$2.939E+02$	$2.314E+02$
F30	AVG	$1.164E+04$	$1.193E+04$	$9.363E+03$	$1.198E+04$	$\mathbf{8.889E+03}$
	STD	$4.169E+03$	$4.785E+03$	$3.365E+03$	$4.627E+03$	$\mathbf{3.232E+03}$
	+/–/=	$\sim$	0/18/11	0/14/15	0/19/10	0/16/13
	Mean	4.448	2.759	2.966	2.310	2.517
	Rank	5	3	4	1	2

3.3 Ablation experiment

Ablation experiment [12] is the most powerful way to verify whether each introduction strategy improves SSA. Therefore, we compare SSA with SSA1 (SSA with hybrid search strategy based on step function is introduced separately), SSA2 (SSA with multi-stage dynamic control factors is introduced separately), SSA3 (SSA for food search strategy based on Logistic model is introduced separately),SSA12(SSA for both hybrid search strategy based on step function and multi-stage dynamic control factors is introduced), SSA13(SSA for both hybrid search strategy based on step function and food search strategy based on Logistic model is introduced), SSA23(SSA for both multi-stage dynamic control factors and food search strategy based on Logistic model is introduced) and MISSA (SSA based on the fusion of three strategies). The ablation experiment is carried out under the same conditions. The number of producers (PD) is set to 30, the safety threshold (S) to 0.6, and the number of scouts (SD) to 50. Table 3 shows the specific parameter settings of the algorithm participating in the ablation experiment.

The results of the Wilcoxon signed-rank test in Table 4 shows that SSA1, SSA2 and SSA3 outperform SSA in terms of 16, 5 and 10 benchmark functions, respectively, while SSA12, SSA13 and SSA23 outperform SSA in terms of 12, 14 and 9 benchmark functions, respectively. Therefore, the introduced three strategies all have a partial improvement on SSA. The optimization performance of MISSA is better than that of SSA in 19 benchmark functions and close to that of SSA in the rest. Therefore, the three strategies introduced at the same time can improve the overall performance of SSA. As can be seen from the p values obtained by Wilcoxon signed-rank test in Table 5, p values on some benchmark functions

Table 2 p-values of SSA and MISSA with different parameter settings based on Wilcoxon test

Fun	MISSA (ub=0.6,lb=0.2)	MISSA (ub=0.6,lb=0.4)	MISSA (ub=0.8,lb=0.2)	MISSA (ub=0.8,lb=0.4)
F1	$1.108E-02$	$\mathbf{1.470E-01}$	$4.716E-02$	$5.318E-03$
F3	$2.125E-06$	$1.733E-06$	$1.731E-06$	$2.121E-06$
F4	$\mathbf{4.165E-01}$	$\mathbf{9.590E-01}$	$1.591E-03$	$\mathbf{7.343E-01}$
F5	$1.477E-02$	$1.471E-04$	$4.803E-03$	$1.035E-03$
F6	$4.194E-04$	$7.271E-03$	$8.241E-04$	$\mathbf{4.528E-01}$
F7	$1.357E-04$	$8.448E-06$	$1.551E-04$	$3.060E-04$
F8	$1.954E-02$	$\mathbf{5.983E-02}$	$\mathbf{5.391E-02}$	$2.560E-02$
F9	$2.152E-05$	$3.880E-06$	$1.919E-06$	$3.494E-06$
F10	$\mathbf{2.133E-01}$	$\mathbf{7.035E-01}$	$\mathbf{1.704E-01}$	$\mathbf{5.707E-02}$
F11	$6.968E-06$	$1.357E-05$	$4.942E-06$	$1.194E-03$
F12	$2.430E-02$	$2.254E-03$	$7.682E-04$	$4.681E-03$
F13	$3.682E-02$	$\mathbf{9.774E-02}$	$2.552E-02$	$1.956E-02$
F14	$6.410E-03$	$\mathbf{1.156E-01}$	$2.215E-03$	$3.852E-03$
F15	$\mathbf{4.047E-01}$	$\mathbf{1.109E-01}$	$\mathbf{7.800E-01}$	$\mathbf{9.918E-01}$
F16	$\mathbf{2.288E-01}$	$\mathbf{3.492E-01}$	$\mathbf{4.765E-01}$	$\mathbf{5.707E-02}$
F17	$9.264E-03$	$5.654E-03$	$1.147E-04$	$1.112E-03$
F18	$3.870E-02$	$\mathbf{5.707E-02}$	$\mathbf{7.504E-02}$	$\mathbf{7.518E-02}$
F19	$1.108E-02$	$2.431E-02$	$4.873E-04$	$8.726E-03$
F20	$4.714E-02$	$\mathbf{4.165E-01}$	$8.120E-03$	$\mathbf{8.581E-02}$
F21	$1.121E-05$	$7.481E-05$	$1.228E-05$	$1.742E-04$
F22	$\mathbf{3.184E-01}$	$\mathbf{3.709E-01}$	$\mathbf{1.311E-01}$	$\mathbf{5.438E-01}$
F23	$\mathbf{6.435E-01}$	$\mathbf{4.405E-01}$	$1.106E-03$	$\mathbf{1.020E-01}$
F24	$1.107E-02$	$4.677E-03$	$1.668E-03$	$2.179E-02$
F25	$\mathbf{5.857E-01}$	$\mathbf{1.413E-01}$	$\mathbf{1.350E-01}$	$\mathbf{8.450E-01}$
F26	$\mathbf{6.143E-01}$	$\mathbf{5.716E-01}$	$\mathbf{4.280E-01}$	$\mathbf{2.059E-01}$
F27	$\mathbf{4.779E-01}$	$\mathbf{5.303E-01}$	$\mathbf{9.260E-01}$	$\mathbf{8.130E-01}$
F28	$\mathbf{5.857E-01}$	$2.765E-03$	$6.414E-03$	$\mathbf{1.254E-01}$
F29	$2.957E-03$	$9.264E-03$	$1.468E-02$	$8.210E-03$
F30	$\mathbf{7.971E-01}$	$1.563E-02$	$\mathbf{4.646E-01}$	$1.478E-02$

are far less than 0.05, which implies that the introduction of one improvement strategy alone or two different improvement strategies at the same time can significantly improve the optimization performance of SSA only in some benchmark functions, while the introduction of three improved strategies at the same time can significantly improve the performance of MISSA in most benchmark functions compared with SSA. According to results of Freidman test, MISSA has the smallest Mean value, followed by SSA13,SSA12, SSA1, SSA23, SSA3 and SSA2, and SSA ranks last. The overall ranking illustrates that the performance of SSA with two strategies introduced simultaneously performs better than that of SSA with two strategies introduced separately, SSA with three strategies introduced simultaneously outperforms that of SSA with three strategies introduced separately, and SSA with three strategies introduced simultaneously achieves the best performance. It also fully demonstrates that the hybrid search strategy based on step function, multi-stage dynamic control

Table 3 Parameter settings of ablation experiment

Algorithm	Parameter settings
SSA1	$p_1 = 0.5$
SSA2	$T_1 = 500, T_2 = 1500, ub = 0.8, lb = 0.2$
SSA3	$G = 4.rand() - 2, w = 0, a = \frac{1}{100}, b = -10$

factor and the food search strategy based on Logistic model can provide great help to the improvement of original SSA.

3.4 Comparison with peer algorithms

In order to evaluate the performance of MISSA comprehensively and objectively, we compare it with gray wolf optimization algorithm [27] (GWO), particle swarm optimization algorithm [19] (PSO), whale optimization algorithm [26] (WOA), artificial bee colony algorithm [17] (ABC), improved sparrow search algorithm [6] (ISSA1), chaotic sparrow search algorithm [49] (CSSA) and improved sparrow search algorithm [45] (ISSA2) to objectively reflect the effectiveness of the improved algorithm. The main parameter settings of each algorithm are shown in Table 6.

According to the results of Wilcoxon sign-rank test in Table 7, compared with the four classical algorithms GWO, PSO, WOA and ABC, MISSA has better optimization results on 19, 13, 29 and 22 benchmark functions respectively. Compared with the three improved algorithms ISSA1, CSSA and ISSA2, MISSA has better results on 29, 19 and 28 benchmark functions respectively. Among them, it is worth explaining that the optimization result of MISSA on CEC2017 benchmark function is completely superior to WOA and ISSA1. As can be seen from the p values obtained by Wilcoxon signed-rank test in Table 8, p values are far less than 0.05 on most benchmark functions, suggesting significant performance differences between MISSA and the algorithms being compared. It can be seen that the p values of MISSA, WOA and ISSA1 are all less than 0.05 in all benchmark functions, so there is a significant gap in their optimization performance. It can be seen from the ranking results of Friedman test in Table 7, MISSA ranks first with Mean value of 1.793, and still has great advantages compared with other algorithms. Therefore, as shown by rank in Table 7, according to the average ranking results, MISSA has the best comprehensive optimization performance, followed by PSO and CSSA. In general, MISSA performs better than other algorithms on most of the CEC2017 benchmark functions, and is only equal to PSO or CSSA on some of the benchmark functions, which reflects powerful optimization ability of MISSA, and also verifies the advantages of MISSA in solving high-dimensional complex function problems.

In order to visualize the convergence behavior of the MISSA algorithm, we select 1 - 2 functions from each of these 4 groups of different functions to verify the performance of the algorithm. For example, F1 represents the unimodal function, F4 represents the simple multi-modal function, F12 and F19 represent the hybrid function, and F22 and F28 represent the composition function. The convergence curves of the nine algorithms for solving unimodal functions, simple multi-modal functions, hybrid functions and composition functions are given in Fig. 3. It can be seen that the early convergence speed of MISSA on F1 and F4 is slower than that of PSO and SSA, but its final convergence accuracy is better than other algorithms. On F12, with the exception of CSSA, SSA and MSSIA, the other algorithms

Table 4 Ablation experiments

Fun	Item	SSA	SSA1	SSA2	SSA3	SSA12	SSA13	SSA23	MISSA
F1	AVG	$6.211E+03$	$8.039E+03$	$4.890E+03$	$8.201E+03$	$7.062E+03$	$5.158E+03$	$5.559E+03$	$\mathbf{4.126E+03}$
	STD	$5.538E+03$	$6.815E+03$	$5.799E+03$	$6.690E+03$	$6.753E+03$	$5.999E+03$	$4.653E+03$	$\mathbf{4.191E+03}$
F3	AVG	$3.059E+03$	$4.263E+03$	$2.000E+03$	$3.499E+02$	$3.510E+03$	$\mathbf{3.432E+02}$	$4.408E+02$	$4.618E+02$
	STD	$1.385E+03$	$2.850E+03$	$9.314E+02$	$1.415E+02$	$1.923E+03$	$3.931E+01$	$1.995E+02$	$\mathbf{1.317E+02}$
F4	AVG	$4.708E+02$	$4.747E+02$	$4.855E+02$	$4.694E+02$	$4.729E+02$	$4.645E+02$	$4.760E+02$	$\mathbf{4.464E+02}$
	STD	$2.845E+01$	$\mathbf{2.095E+01}$	$2.419E+01$	$2.187E+01$	$3.003E+01$	$3.301E+01$	$2.413E+01$	$3.161E+01$
F5	AVG	$7.189E+02$	$6.805E+02$	$7.241E+02$	$7.253E+02$	$\mathbf{6.729E+02}$	$6.776E+02$	$7.601E+02$	$6.880E+02$
	STD	$3.381E+01$	$4.773E+01$	$5.098E+01$	$5.538E+01$	$3.798E+01$	$4.608E+01$	$6.909E+01$	$\mathbf{3.051E+01}$
F6	AVG	$6.414E+02$	$\mathbf{6.252E+02}$	$6.392E+02$	$6.436E+02$	$6.262E+02$	$6.304E+02$	$6.569E+02$	$6.292E+02$
	STD	$\mathbf{8.634E+00}$	$9.302E+00$	$1.033E+01$	$8.421E+00$	$1.025E+01$	$1.136E+01$	$9.358E+00$	$1.149E+01$
F7	AVG	$1.152E+03$	$1.025E+03$	$1.160E+03$	$1.057E+03$	$1.047E+03$	$\mathbf{1.014E+03}$	$1.037E+03$	$1.017E+03$
	STD	$1.087E+02$	$1.081E+02$	$1.187E+02$	$\mathbf{6.833E+01}$	$1.333E+02$	$9.791E+01$	$7.356E+01$	$7.972E+01$
F8	AVG	$9.554E+02$	$9.506E+02$	$9.751E+02$	$1.013E+03$	$9.474E+02$	$\mathbf{9.406E+02}$	$1.004E+03$	$9.420E+02$
	STD	$3.057E+01$	$3.073E+01$	$2.534E+01$	$4.970E+01$	$3.180E+01$	$2.350E+01$	$4.967E+01$	$\mathbf{1.862E+01}$
F9	AVG	$5.201E+03$	$4.433E+03$	$5.286E+03$	$7.099E+03$	$4.316E+03$	$\mathbf{3.496E+03}$	$6.435E+03$	$3.528E+03$
	STD	$5.874E+02$	$\mathbf{1.926E+02}$	$2.252E+02$	$1.387E+03$	$1.122E+03$	$9.133E+02$	$1.675E+03$	$7.408E+02$
F10	AVG	$5.155E+03$	$\mathbf{4.517E+03}$	$4.897E+03$	$5.327E+03$	$4.920E+03$	$5.080E+03$	$5.314E+03$	$4.964E+03$
	STD	$\mathbf{5.204E+02}$	$6.872E+02$	$8.399E+02$	$6.376E+02$	$5.705E+02$	$6.591E+02$	$6.489E+02$	$6.188E+02$
F11	AVG	$1.355E+03$	$\mathbf{1.210E+03}$	$1.371E+03$	$1.353E+03$	$1.254E+03$	$1.243E+03$	$1.363E+03$	$1.245E+03$
	STD	$7.106E+01$	$7.188E+01$	$1.028E+02$	$1.011E+02$	$8.049E+01$	$6.848E+01$	$1.031E+02$	$\mathbf{6.596E+01}$
F12	AVG	$1.146E+05$	$1.136E+05$	$1.228E+05$	$7.305E+04$	$1.018E+05$	$6.320E+04$	$5.399E+04$	$\mathbf{6.527E+04}$
	STD	$5.794E+04$	$7.748E+04$	$5.999E+04$	$\mathbf{2.548E+04}$	$5.034E+04$	$2.726E+04$	$2.973E+04$	$3.313E+04$
F13	AVG	$3.020E+04$	$1.894E+04$	$2.194E+04$	$1.607E+04$	$2.271E+04$	$1.610E+04$	$\mathbf{1.345E+04}$	$1.503E+04$
	STD	$2.601E+04$	$2.407E+04$	$2.172E+04$	$1.882E+04$	$2.079E+04$	$2.074E+04$	$\mathbf{1.386E+04}$	$1.614E+04$

Table 4 (continued)

Fun	Item	SSA	SSA1	SSA2	SSA3	SSA12	SSA13	SSA23	MISSA
F14	AVG	$1.323E+04$	$1.161E+04$	$1.179E+04$	$9.578E+03$	$1.142E+04$	$6.921E+03$	$\mathbf{5.632E+03}$	$8.056E+03$
	STD	$6.732E+03$	$9.692E+03$	$5.920E+03$	$6.011E+03$	$8.515E+03$	$3.814E+03$	$\mathbf{2.524E+03}$	$4.037E+03$
F15	AVG	$1.181E+04$	$1.481E+04$	$1.852E+04$	$1.013E+04$	$1.317E+04$	$\mathbf{9.576E+03}$	$1.120E+04$	$1.140E+04$
	STD	$1.175E+04$	$1.185E+04$	$1.369E+04$	$1.046E+04$	$1.413E+04$	$1.027E+04$	$\mathbf{8.862E+03}$	$1.380E+04$
F16	AVG	$2.879E+03$	$2.797E+03$	$2.805E+03$	$2.930E+03$	$2.684E+03$	$\mathbf{2.660E+03}$	$2.861E+03$	$2.792E+03$
	STD	$2.748E+02$	$3.293E+02$	$3.311E+02$	$4.398E+02$	$3.210E+02$	$2.778E+02$	$3.443E+02$	$\mathbf{2.076E+02}$
F17	AVG	$2.537E+03$	$2.343E+03$	$2.495E+03$	$2.384E+03$	$2.327E+03$	$2.369E+03$	$\mathbf{2.171E+03}$	$2.286E+03$
	STD	$\mathbf{1.779E+02}$	$2.205E+02$	$2.009E+02$	$2.212E+02$	$2.295E+02$	$1.936E+02$	$3.436E+02$	$1.784E+02$
F18	AVG	$2.940E+05$	$1.415E+05$	$2.454E+05$	$9.907E+04$	$1.927E+05$	$1.972E+05$	$\mathbf{8.995E+04}$	$2.001E+05$
	STD	$2.457E+05$	$1.460E+05$	$2.193E+05$	$8.748E+04$	$1.897E+05$	$1.447E+05$	$\mathbf{6.241E+04}$	$1.389E+05$
F19	AVG	$2.421E+04$	$1.023E+04$	$9.693E+03$	$1.358E+04$	$9.100E+03$	$9.721E+03$	$2.309E+04$	$\mathbf{6.410E+03}$
	Std	$2.282E+04$	$2.106E+04$	$1.233E+04$	$1.774E+04$	$9.762E+03$	$1.056E+04$	$1.827E+04$	$\mathbf{8.787E+03}$
F20	AVG	$2.633E+03$	$2.473E+03$	$2.653E+03$	$2.761E+03$	$2.459E+03$	$2.571E+03$	$2.612E+03$	$\mathbf{2.253E+03}$
	STD	$1.975E+02$	$1.843E+02$	$2.221E+02$	$2.942E+02$	$1.824E+02$	$\mathbf{1.803E+02}$	$3.009E+02$	$1.977E+02$
F21	AVG	$2.518E+03$	$2.438E+03$	$2.512E+03$	$2.507E+03$	$\mathbf{2.435E+03}$	$2.454E+03$	$2.544E+03$	$2.453E+03$
	STD	$5.873E+01$	$4.426E+01$	$5.248E+01$	$3.717E+01$	$3.099E+01$	$3.235E+01$	$4.539E+01$	$\mathbf{2.635E+01}$
F22	AVG	$4.224E+03$	$5.055E+03$	$6.024E+03$	$6.045E+03$	$3.656E+03$	$3.845E+03$	$6.547E+03$	$\mathbf{3.136E+03}$
	STD	$2.297E+03$	$1.992E+03$	$1.592E+03$	$1.773E+03$	$2.127E+03$	$2.248E+03$	$\mathbf{1.296E+03}$	$1.724E+03$
F23	AVG	$2.866E+03$	$2.834E+03$	$2.857E+03$	$2.862E+03$	$2.856E+03$	$2.848E+03$	$2.837E+03$	$\mathbf{2.822E+03}$
	STD	$4.608E+01$	$6.505E+01$	$5.182E+01$	$6.464E+01$	$7.114E+01$	$5.779E+01$	$6.970E+01$	$\mathbf{4.474E+01}$
F24	AVG	$3.077E+03$	$3.034E+03$	$3.024E+03$	$3.017E+03$	$3.009E+03$	$\mathbf{3.000E+03}$	$3.022E+03$	$3.011E+03$
	STD	$8.673E+01$	$6.644E+01$	$7.143E+01$	$\mathbf{4.158E+01}$	$5.141E+01$	$6.786E+01$	$4.920E+01$	$4.244E+01$

Table 4 (continued)

Fun	Item	SSA	SSA1	SSA2	SSA3	SSA12	SSA13	SSA23	MISSA
F25	AVG	$2.890E+03$	$2.891E+03$	$2.902E+03$	$2.899E+03$	$2.891E+03$	$2.889E+03$	$2.889E+03$	$\mathbf{2.888E+03}$
	STD	$\mathbf{7.374E+00}$	$2.118E+01$	$1.885E+01$	$2.002E+01$	$1.216E+01$	$9.327E+00$	$1.085E+01$	$8.184E+00$
F26	AVG	$5.803E+03$	$5.058E+03$	$6.188E+03$	$5.508E+03$	$5.625E+03$	$5.652E+03$	$\mathbf{5.002E+03}$	$5.919E+03$
	STD	$9.018E+02$	$1.080E+03$	$\mathbf{8.087E+02}$	$9.258E+02$	$1.331E+03$	$1.413E+03$	$1.906E+03$	$9.675E+02$
F27	AVG	$3.248E+03$	$3.278E+03$	$3.250E+03$	$3.249E+03$	$3.265E+03$	$3.265E+03$	$3.264E+03$	$\mathbf{3.245E+03}$
	STD	$2.246E+01$	$2.446E+01$	$\mathbf{1.805E+01}$	$2.893E+01$	$4.149E+01$	$3.797E+01$	$2.583E+01$	$1.873E+01$
F28	AVG	$3.183E+03$	$3.149E+03$	$3.135E+03$	$3.164E+03$	$3.171E+03$	$3.154E+03$	$3.167E+03$	$\mathbf{3.135E+03}$
	STD	$\mathbf{5.519E+01}$	$6.551E+01$	$5.733E+01$	$7.674E+01$	$6.832E+01$	$6.783E+01$	$7.409E+01$	$5.983E+01$
F29	AVG	$4.187E+03$	$4.046E+03$	$4.041E+03$	$4.053E+03$	$\mathbf{3.988E+03}$	$4.106E+03$	$4.213E+03$	$4.043E+03$
	STD	$2.684E+02$	$3.293E+02$	$2.451E+02$	$2.223E+02$	$2.815E+02$	$2.833E+02$	$\mathbf{2.090E+02}$	$2.939E+02$
F30	AVG	$1.164E+04$	$1.319E+04$	$\mathbf{9.904E+03}$	$1.176E+04$	$1.087E+04$	$9.970E+03$	$1.266E+04$	$1.198E+04$
	STD	$4.169E+03$	$4.263E+03$	$4.421E+03$	$5.942E+03$	$4.894E+03$	$4.202E+03$	$\mathbf{3.984E+03}$	$4.627E+03$
	+/-/=	$\sim$	2/16/11	4/5/20	3/10/16	0/12/17	1/14/14	7/9/13	0/19/10
	Mean	6.207	4.379	5.690	5.310	3.897	3.000	4.931	2.586
	Rank	8	4	7	6	3	2	5	1

Table 5 The p value of SSA and improvement strategy based on Wilcoxon test

Fun	SSA1	SSA2	SSA3	SSA12	SSA13	SSA23	MISSA
F1	$\mathbf{9.775E-02}$	$\mathbf{2.895E-01}$	$5.653E-03$	$\mathbf{6.884E-01}$	$\mathbf{3.820E-01}$	$\mathbf{5.856E-01}$	$4.716E-02$
F3	$7.019E-03$	$2.582E-03$	$2.807E-04$	$\mathbf{4.165E-01}$	$1.920E-06$	$2.310E-06$	$1.731E-06$
F4	$\mathbf{9.754E-01}$	$4.491E-02$	$2.696E-02$	$\mathbf{8.130E-01}$	$\mathbf{4.528E-01}$	$\mathbf{7.811E-01}$	$1.591E-03$
F5	$4.118E-05$	$\mathbf{2.536E-01}$	$\mathbf{1.966E-01}$	$1.598E-04$	$1.962E-03$	$2.541E-02$	$4.803E-03$
F6	$5.124E-06$	$\mathbf{4.653E-01}$	$2.557E-02$	$2.594E-05$	$5.287E-04$	$1.013E-05$	$8.241E-04$
F7	$3.590E-03$	$\mathbf{4.907E-01}$	$\mathbf{5.901E-02}$	$6.022E-03$	$6.154E-04$	$5.185E-04$	$1.551E-04$
F8	$\mathbf{6.578E-01}$	$1.044E-02$	$\mathbf{1.836E-01}$	$\mathbf{3.184E-01}$	$\mathbf{7.190E-02}$	$4.001E-05$	$\mathbf{5.391E-02}$
F9	$4.347E-04$	$\mathbf{5.716E-01}$	$\mathbf{1.342E-01}$	$4.527E-04$	$1.969E-05$	$1.407E-04$	$1.919E-06$
F10	$1.804E-04$	$\mathbf{1.846E-01}$	$\mathbf{5.852E-01}$	$\mathbf{1.109E-01}$	$\mathbf{5.856E-01}$	$\mathbf{6.286E-01}$	$\mathbf{1.704E-01}$
F11	$5.939E-06$	$\mathbf{5.715E-01}$	$\mathbf{7.023E-01}$	$2.048E-04$	$3.717E-05$	$\mathbf{9.918E-01}$	$4.942E-06$
F12	$\mathbf{5.855E-01}$	$\mathbf{4.284E-01}$	$\mathbf{4.154E-01}$	$\mathbf{4.048E-01}$	$4.895E-04$	$1.727E-04$	$7.682E-04$
F13	$\mathbf{1.252E-01}$	$\mathbf{1.588E-01}$	$4.937E-02$	$\mathbf{3.185E-01}$	$1.244E-02$	$8.694E-03$	$2.552E-02$
F14	$\mathbf{2.274E-01}$	$\mathbf{2.989E-01}$	$4.120E-02$	$\mathbf{1.413E-01}$	$2.829E-04$	$1.031E-05$	$2.215E-03$
F15	$\mathbf{5.020E-01}$	$\mathbf{9.359E-02}$	$\mathbf{6.446E-02}$	$\mathbf{7.812E-01}$	$\mathbf{5.440E-01}$	$\mathbf{9.588E-01}$	$\mathbf{7.800E-01}$

Table 5 (continued)

Fun	SSA1	SSA2	SSA3	SSA12	SSA13	SSA23	MISSA
F16	**1.044E − 01**	**5.998E − 01**	**6.410E − 01**	2.430E − 02	9.264E − 03	**8.449E − 01**	**4.765E − 01**
F17	1.827E − 04	**4.284E − 01**	1.454E − 03	2.757E − 03	4.190E − 04	2.087E − 04	1.147E − 04
F18	3.654E − 02	**4.048E − 01**	**1.911E − 01**	**9.774E − 02**	**1.986E − 01**	8.776E − 04	**7.504E − 02**
F19	2.832E − 02	5.665E − 03	**2.704E − 01**	1.197E − 03	1.397E − 02	**6.140E − 01**	4.873E − 04
F20	1.542E − 02	**7.655E − 01**	1.542E − 02	4.390E − 03	**1.254E − 01**	**6.728E − 01**	8.120E − 03
F21	3.246E − 05	**9.754E − 01**	3.996E − 03	5.214E − 06	8.903E − 05	1.521E − 02	1.228E − 05
F22	**4.249E − 01**	1.106E − 02	1.574E − 03	**6.425E − 01**	**9.426E − 01**	1.539E − 03	**1.311E − 01**
F23	3.789E − 03	**4.907E − 01**	**5.694E − 01**	**5.999E − 01**	**1.650E − 01**	**7.100E − 02**	1.106E − 03
F24	9.042E − 03	1.851E − 02	**2.701E − 01**	2.765E − 03	6.154E − 04	1.382E − 02	1.668E − 03
F25	**4.883E − 01**	4.388E − 03	**2.195E − 01**	**8.290E − 01**	**1.155E − 01**	**1.140E − 01**	**1.350E − 01**
F26	5.214E − 03	**9.367E − 02**	**8.611E − 01**	**8.774E − 01**	**7.971E − 01**	3.460E − 02	**4.280E − 01**
F27	1.405E − 02	**6.435E − 01**	**4.138E − 01**	**1.588E − 01**	4.715E − 02	6.595E − 03	**9.260E − 01**
F28	2.997E − 02	1.245E − 02	2.177E − 02	**5.999E − 01**	**1.109E − 01**	**4.404E − 01**	6.414E − 03
F29	2.162E − 02	1.849E − 02	2.517E − 02	1.108E − 02	**1.470E − 01**	**8.126E − 01**	1.468E − 02
F30	**7.503E − 02**	**1.306E − 01**	3.092E − 03	**4.165E − 01**	**1.064E − 01**	**1.354E − 01**	**4.646E − 01**

Table 6 Main parameters of the algorithm

Algorithm	Parameter settings
GWO	$A = 2a.r_1 - a; a(t) = 2 - 2.\frac{2t}{T_{max}}, C = 2.r_2$
PSO	$c_1 = 2; c_2 = 2; w = 0.729$
WOA	$b = 1; a = 2 - \frac{2t}{T_{max}}, p^* = 0.5$
ABC	$L = round(0.6 * dim * N); a = 1$
ISSA1	$PD = 30, SD = 50, S = 0.6, N = 1 - \frac{2t}{T_{max}}$
CSSA	$PD = 30, SD = 70 - round(\frac{(70-50).t}{T_{max}}), S = 0.6$
ISSA2	$PD = 30, SD = 50, S = 0.6, w = \frac{e^{2.(1-\frac{t}{T_{max}})} - e^{-2.(1-\frac{t}{T_{max}})}}{e^{2.(1-\frac{t}{T_{max}})} + e^{-2.(1-\frac{t}{T_{max}})}}$

converge to the suboptimal solution early, but the convergence accuracy and convergence speed of MISSA are obviously better than CSSA and SSA. On F19, F22 and F28, compared with other algorithms, it can be found that the convergence curve of MISSA drops faster and can converge to a solution with higher precision.

In the actual optimization process of SSA, convergence to suboptimal solution often occurs. A remarkable feature of populations trapped in local optimal solutions is that there is little difference between individuals. Therefore, when the difference between individuals is small, the population is more likely to fall into the local optimal solution. Evaluating population diversity correctly is a measure of the ability of the algorithm to escape the local optimal solution. In this paper, the diversity of the sparrow population at the t-th iteration is calculated as follows [23]:

$$S(t) = \frac{1}{N}\sum_{i=1}^{N}\sqrt{\sum_{j=1}^{D}(x_{i,j}(t) - \bar{x}_j(t))^2} \tag{21}$$

Where D is the dimension of optimization problem, N is the population size of sparrow, $x_{i,j}(t)$ represents the position of the i-th sparrow on the j-th dimensional optimization problem at the t-th iteration, $\bar{x}_j(t)$ represents the average position of the t-th generation population.

Figure 4 shows the population diversity of SSA and MISSA, where the abscissa represents the maximum evaluation times and the ordinate represents the diversity value of the population. It can be found that at the initial stage of the population, the population diversity value of MISSA is greater than that of SSA, which means that the diversity of the initial population of MISSA is better than that of SSA. In the middle of iteration, the population diversity values of SSA and MISSA decreased with the increase of iteration times. It is worth noting that the diversity value of SSA has long remained at a position greater than 10 and fluctuated slightly, indicating that the population of SSA converges to a certain region of the search space, while MISSA still oscillates downward. At the end of iteration, the population diversity value of MISSA proposed by us fluctuates greatly at about 1, which means that MISSA still has the ability to escape the local optimal solution at the end of iteration.

Table 7 Comparison of optimization results of each algorithm

Fun	Item	MISSA	GWO	PSO	WOA	ABC	ISSA1	CSSA	ISSA2
F1	AVG	$\mathbf{4.126E+03}$	$3.438E+09$	$8.055E+03$	$7.840E+04$	$2.147E+05$	$4.876E+10$	$4.278E+03$	$7.930E+10$
	STD	$\mathbf{4.191E+03}$	$6.334E+07$	$6.368E+03$	$2.420E+04$	$1.519E+05$	$1.157E+10$	$4.395E+03$	$1.128E+09$
F3	AVG	$4.618E+02$	$3.046E+04$	$\mathbf{3.202E+02}$	$1.240E+05$	$2.976E+05$	$9.409E+04$	$1.521E+04$	$8.895E+04$
	STD	$1.317E+02$	$6.130E+03$	$\mathbf{4.717E+00}$	$6.867E+04$	$4.009E+04$	$5.727E+02$	$4.417E+03$	$3.109E+03$
F4	AVG	$\mathbf{4.464E+02}$	$6.741E+02$	$4.703E+02$	$5.030E+02$	$4.504E+02$	$1.206E+03$	$4.828E+02$	$1.799E+04$
	STD	$3.161E+01$	$5.223E+01$	$\mathbf{1.742E+01}$	$2.875E+01$	$3.023E+01$	$2.885E+03$	$2.255E+01$	$2.292E+03$
F5	AVG	$\mathbf{6.880E+02}$	$7.009E+02$	$6.881E+02$	$7.493E+02$	$7.146E+02$	$9.746E+02$	$7.400E+02$	$9.926E+02$
	STD	$3.051E+01$	$1.351E+01$	$4.474E+01$	$6.816E+01$	$\mathbf{9.158E+00}$	$3.902E+01$	$5.525E+01$	$1.846E+01$
F6	AVG	$6.292E+02$	$6.255E+02$	$6.505E+02$	$6.618E+02$	$\mathbf{6.005E+02}$	$7.012E+02$	$6.314E+02$	$7.009E+02$
	STD	$1.149E+01$	$2.328E+00$	$6.947E+00$	$6.688E+00$	$\mathbf{5.767E-02}$	$8.013E+00$	$1.479E+01$	$4.996E+00$
F7	AVG	$1.017E+03$	$9.713E+02$	$1.007E+03$	$1.188E+03$	$\mathbf{9.566E+02}$	$1.512E+03$	$1.074E+03$	$1.487E+03$
	STD	$7.972E+01$	$1.922E+01$	$6.147E+01$	$9.056E+01$	$\mathbf{9.230E+00}$	$5.320E+01$	$1.167E+02$	$1.388E+01$
F8	AVG	$9.420E+02$	$9.888E+02$	$\pm 9.351E+02$	$1.007E+03$	$1.023E+03$	$1.212E+03$	$9.963E+02$	$1.205E+03$
	STD	$1.862E+01$	$1.124E+01$	$2.758E+01$	$3.661E+01$	$\mathbf{8.568E+00}$	$2.502E+01$	$3.767E+01$	$1.025E+01$
F9	AVG	$3.528E+03$	$2.438E+03$	$4.108E+03$	$7.207E+03$	$\mathbf{1.153E+03}$	$1.612E+04$	$4.913E+03$	$1.312E+04$
	STD	$7.408E+02$	$5.388E+02$	$4.979E+02$	$2.121E+03$	$\mathbf{7.503E+01}$	$1.122E+03$	$6.823E+02$	$1.267E+03$
F10	AVG	$\mathbf{4.964E+03}$	$7.264E+03$	$5.117E+03$	$5.928E+03$	$8.829E+03$	$8.562E+03$	$5.353E+03$	$9.701E+03$
	STD	$6.188E+02$	$7.059E+02$	$4.812E+02$	$1.138E+03$	$3.136E+02$	$\mathbf{1.785E+02}$	$5.992E+02$	$4.694E+02$
F11	AVG	$1.245E+03$	$1.688E+03$	$\mathbf{1.222E+03}$	$1.324E+03$	$5.033E+03$	$1.317E+04$	$1.305E+03$	$9.632E+03$
	STD	$6.596E+01$	$5.498E+02$	$\mathbf{2.236E+01}$	$6.038E+01$	$1.094E+03$	$2.138E+03$	$7.643E+01$	$8.612E+02$
F12	AVG	$\mathbf{6.527E+04}$	$2.703E+08$	$4.649E+05$	$2.083E+07$	$2.697E+08$	$6.247E+09$	$1.336E+05$	$2.401E+10$
	STD	$\mathbf{3.313E+04}$	$6.640E+07$	$3.397E+05$	$1.965E+07$	$6.480E+07$	$1.922E+09$	$1.121E+05$	$1.447E+09$
F13	AVG	$1.503E+04$	$1.172E+08$	$\mathbf{1.455E+04}$	$1.388E+05$	$2.299E+05$	$2.894E+09$	$3.196E+04$	$1.885E+10$
	STD	$1.614E+04$	$4.794E+07$	$\mathbf{1.118E+04}$	$6.258E+04$	$7.943E+05$	$2.331E+09$	$2.070E+04$	$2.097E+09$

Table 7 (continued)

Fun	Item	MISSA	GWO	PSO	WOA	ABC	ISSA1	CSSA	ISSA2
F14	AVG	$8.056E+03$	$1.206E+05$	$\mathbf{7.651E+03}$	$1.530E+05$	$1.660E+05$	$4.456E+06$	$1.891E+04$	$1.174E+04$
	STD	$\mathbf{4.037E+03}$	$1.504E+05$	$4.956E+03$	$1.652E+05$	$6.326E+04$	$3.454E+06$	$1.013E+04$	$7.482E+03$
F15	AVG	$1.140E+04$	$1.757E+06$	$\mathbf{6.263E+03}$	$7.471E+04$	$8.379E+05$	$5.490E+08$	$2.727E+04$	$3.653E+09$
	STD	$1.380E+04$	$1.477E+06$	$\mathbf{7.081E+03}$	$5.638E+04$	$3.758E+05$	$3.963E+08$	$1.649E+04$	$7.378E+08$
F16	AVG	$2.792E+03$	$\mathbf{2.700E+03}$	$2.929E+03$	$3.429E+03$	$3.583E+03$	$4.540E+03$	$2.842E+03$	$1.144E+04$
	STD	$2.076E+02$	$2.588E+02$	$3.608E+02$	$4.690E+02$	$\mathbf{1.727E+02}$	$1.942E+02$	$3.243E+02$	$2.692E+03$
F17	AVG	$2.286E+03$	$\mathbf{2.144E+03}$	$2.381E+03$	$2.401E+03$	$2.751E+03$	$3.541E+03$	$2.268E+03$	$2.424E+04$
	STD	$1.784E+02$	$\mathbf{1.579E+02}$	$2.518E+02$	$1.916E+02$	$1.075E+02$	$3.581E+02$	$2.478E+02$	$5.048E+04$
F18	AVG	$\mathbf{2.001E+05}$	$8.475E+05$	$2.418E+05$	$1.530E+06$	$7.490E+06$	$5.645E+07$	$2.435E+05$	$1.401E+06$
	STD	$\mathbf{1.389E+05}$	$6.233E+05$	$1.760E+05$	$1.677E+06$	$2.803E+06$	$2.094E+07$	$1.879E+05$	$1.907E+06$
F19	AVG	$\mathbf{6.410E+03}$	$4.022E+06$	$1.188E+04$	$2.400E+06$	$1.766E+04$	$5.631E+08$	$1.303E+04$	$1.681E+08$
	STD	$\mathbf{8.787E+03}$	$2.396E+06$	$9.453E+03$	$1.761E+06$	$1.835E+04$	$4.960E+08$	$1.138E+04$	$1.916E+08$
F20	AVG	$\mathbf{2.253E+03}$	$2.471E+03$	$2.726E+03$	$2.610E+03$	$2.844E+03$	$3.303E+03$	$2.685E+03$	$3.086E+03$
	STD	$1.977E+02$	$1.351E+02$	$2.095E+02$	$1.151E+02$	$8.714E+01$	$\mathbf{8.147E+01}$	$1.448E+02$	$2.327E+02$
F21	AVG	$\mathbf{2.453E+03}$	$2.463E+03$	$2.473E+03$	$2.549E+03$	$2.517E+03$	$2.692E+03$	$2.496E+03$	$2.951E+03$
	STD	$2.635E+01$	$2.278E+01$	$2.507E+01$	$4.107E+01$	$\mathbf{1.604E+01}$	$3.385E+01$	$3.824E+01$	$2.960E+01$
F22	AVG	$\mathbf{3.136E+03}$	$6.528E+03$	$5.252E+03$	$6.516E+03$	$1.007E+04$	$9.056E+03$	$6.716E+03$	$1.101E+04$
	STD	$1.724E+03$	$2.885E+03$	$2.192E+03$	$1.863E+03$	$\mathbf{2.425E+02}$	$1.541E+03$	$6.868E+02$	$6.748E+02$
F23	AVG	$\mathbf{2.822E+03}$	$2.864E+03$	$3.222E+03$	$3.050E+03$	$2.869E+03$	$3.149E+03$	$2.872E+03$	$3.843E+03$
	STD	$4.474E+01$	$1.278E+01$	$1.740E+02$	$8.386E+01$	$\mathbf{1.162E+01}$	$4.984E+01$	$5.137E+01$	$2.145E+02$

Table 7 (continued)

Fun	Item	MISSA	GWO	PSO	WOA	ABC	ISSA1	CSSA	ISSA2
F24	AVG	**3.011*E* + 03**	3.034*E* + 03	3.338*E* + 03	3.168*E* + 03	3.055*E* + 03	3.286*E* + 03	3.023*E* + 03	4.643*E* + 03
	STD	4.244*E* + 01	1.513*E* + 01	1.084*E* + 02	6.386*E* + 01	**9.486*E* + 00**	4.146*E* + 01	3.489*E* + 01	2.415*E* + 02
F25	AVG	**2.888*E* + 03**	3.009*E* + 03	2.880*E* + 03	2.926*E* + 03	2.885*E* + 03	5.180*E* + 03	2.894*E* + 03	5.584*E* + 03
	STD	8.184*E* + 00	1.736*E* + 01	3.849*E* + 00	2.934*E* + 01	**2.869*E* + 00**	7.766*E* + 02	1.483*E* + 01	3.502*E* + 02
F26	AVG	5.919*E* + 03	5.765*E* + 03	6.595*E* + 03	7.966*E* + 03	**5.529*E* + 03**	9.477*E* + 03	6.065*E* + 03	1.259*E* + 04
	STD	9.675*E* + 02	2.111*E* + 02	2.073*E* + 03	6.356*E* + 02	**1.297*E* + 02**	9.665*E* + 02	4.944*E* + 02	2.187*E* + 02
F27	AVG	3.245*E* + 03	3.260*E* + 03	3.482*E* + 03	3.368*E* + 03	**3.200*E* + 03**	3.506*E* + 03	3.245*E* + 03	6.200*E* + 03
	STD	1.873*E* + 01	2.118*E* + 01	3.624*E* + 02	7.708*E* + 01	**4.590*E* − 05**	5.673*E* + 01	2.607*E* + 01	1.487*E* + 03
F28	AVG	**3.135*E* + 03**	3.468*E* + 03	3.212*E* + 03	3.270*E* + 03	3.300*E* + 03	7.202*E* + 03	3.170*E* + 03	9.303*E* + 03
	STD	5.983*E* + 01	1.005*E* + 02	3.079*E* + 01	2.236*E* + 01	**1.386*E* + 00**	7.067*E* + 02	6.342*E* + 01	1.059*E* + 02
F29	AVG	4.043*E* + 03	**4.006*E* + 03**	4.093*E* + 03	5.012*E* + 03	4.674*E* + 03	5.471*E* + 03	4.069*E* + 03	8.691*E* + 03
	STD	2.939*E* + 02	**1.460*E* + 02**	3.695*E* + 02	6.281*E* + 02	1.954*E* + 02	2.447*E* + 02	2.787*E* + 02	1.609*E* + 02
F30	AVG	1.198*E* + 04	2.755*E* + 07	**1.039*E* + 04**	7.541*E* + 06	1.112*E* + 05	6.170*E* + 08	1.286*E* + 04	8.974*E* + 09
	STD	4.627*E* + 03	9.933*E* + 06	4.283*E* + 03	8.146*E* + 06	4.674*E* + 04	3.887*E* + 08	**4.240*E* + 03**	1.084*E* + 09
	+/-/=	∼	19/4/6	13/2/14	29/0/0	22/6/1	29/0/0	19/0/10	28/0/1
	Mean	1.793	3.828	2.966	5.000	4.483	7.103	3.448	7.379
	Rank	1	4	2	6	5	7	3	8

Table 8 The p value of SSA and improvement strategy based on Wilcoxon test

Fun	GWO	PSO	WOA	ABC	ISSA1	CSSA	ISSA2
F1	$1.732E-06$	$2.562E-02$	$1.726E-06$	$1.732E-06$	$1.728E-06$	$\mathbf{9.918E-01}$	$1.733E-06$
F3	$1.605E-06$	$1.606E-06$	$1.562E-06$	$1.508E-06$	$1.507E-06$	$1.561E-06$	$1.686E-06$
F4	$1.733E-06$	$1.708E-03$	$5.748E-06$	$\mathbf{9.099E-01}$	$1.733E-06$	$4.068E-05$	$1.733E-06$
F5	$\mathbf{6.750E-02}$	$\mathbf{9.261E-01}$	$1.494E-03$	$3.360E-03$	$1.603E-06$	$1.330E-05$	$1.561E-06$
F6	$\mathbf{1.579E-01}$	$8.079E-06$	$1.731E-06$	$1.686E-06$	$1.562E-06$	$\mathbf{3.385E-01}$	$1.692E-06$
F7	$1.363E-03$	$\mathbf{6.132E-01}$	$3.488E-06$	$3.214E-05$	$1.561E-06$	$2.541E-02$	$1.702E-06$
F8	$1.969E-06$	$\mathbf{1.346E-01}$	$1.672E-06$	$1.717E-06$	$1.602E-06$	$7.723E-06$	$1.634E-06$
F9	$8.981E-06$	$2.540E-03$	$1.691E-06$	$1.606E-06$	$1.670E-06$	$1.160E-05$	$1.691E-06$
F10	$2.732E-06$	$\mathbf{1.648E-01}$	$3.593E-03$	$1.643E-06$	$1.643E-06$	$3.811E-02$	$1.701E-06$
F11	$1.698E-06$	$\mathbf{9.719E-02}$	$5.551E-05$	$1.641E-06$	$1.670E-06$	$1.982E-04$	$1.686E-06$
F12	$1.732E-06$	$3.165E-06$	$1.725E-06$	$1.728E-06$	$1.729E-06$	$5.689E-04$	$1.730E-06$
F13	$1.675E-06$	$\mathbf{2.696E-01}$	$2.602E-06$	$2.606E-04$	$1.445E-06$	$7.739E-03$	$1.641E-06$
F14	$1.701E-06$	$\mathbf{7.652E-01}$	$7.501E-06$	$1.697E-06$	$1.695E-06$	$2.099E-05$	$8.629E-03$
F15	$1.670E-06$	$\mathbf{1.101E-01}$	$2.599E-06$	$1.692E-06$	$1.695E-06$	$1.414E-03$	$1.708E-06$
F16	$\mathbf{1.836E-01}$	$2.026E-02$	$8.282E-06$	$1.701E-06$	$1.669E-06$	$\mathbf{6.573E-01}$	$1.603E-06$
F17	$7.152E-04$	$\mathbf{6.267E-02}$	$5.661E-03$	$1.732E-06$	$1.732E-06$	$\mathbf{5.857E-01}$	$1.728E-06$
F18	$3.073E-06$	$\mathbf{2.532E-01}$	$2.539E-06$	$1.709E-06$	$1.669E-06$	$\mathbf{7.969E-01}$	$\mathbf{4.162E-01}$
F19	$1.731E-06$	$2.951E-03$	$1.731E-06$	$1.887E-04$	$1.728E-06$	$3.377E-03$	$1.713E-06$
F20	$\mathbf{8.517E-02}$	$2.202E-03$	$5.958E-03$	$7.324E-06$	$1.673E-06$	$4.946E-03$	$1.644E-06$
F21	$\mathbf{2.893E-01}$	$1.041E-02$	$1.907E-06$	$1.728E-06$	$1.728E-06$	$1.050E-04$	$1.728E-06$
F22	$7.478E-05$	$2.824E-04$	$2.815E-06$	$1.727E-06$	$1.721E-06$	$2.844E-06$	$1.722E-06$
F23	$1.141E-04$	$1.708E-06$	$1.707E-06$	$1.952E-05$	$1.718E-06$	$3.296E-04$	$1.722E-06$
F24	$5.817E-03$	$1.644E-06$	$1.673E-06$	$2.622E-05$	$1.672E-06$	$\mathbf{1.976E-01}$	$1.643E-06$
F25	$1.712E-06$	$2.341E-05$	$5.479E-06$	$5.984E-04$	$1.673E-06$	$8.692E-03$	$1.645E-06$
F26	$2.384E-02$	$\mathbf{2.056E-01}$	$1.669E-06$	$1.240E-03$	$1.704E-06$	$\mathbf{7.183E-01}$	$1.691E-06$
F27	$2.409E-02$	$\mathbf{6.209E-02}$	$1.685E-06$	$1.608E-06$	$1.606E-06$	$\mathbf{3.264E-01}$	$1.691E-06$
F28	$1.726E-06$	$8.135E-05$	$3.486E-06$	$1.711E-06$	$1.707E-06$	$1.106E-02$	$1.728E-06$
F29	$\mathbf{5.165E-01}$	$\mathbf{5.715E-01}$	$1.896E-06$	$1.725E-06$	$1.712E-06$	$\mathbf{5.036E-01}$	$1.686E-06$
F30	$1.645E-06$	$\mathbf{2.203E-01}$	$1.672E-06$	$1.645E-06$	$1.644E-06$	$\mathbf{5.849E-01}$	$1.644E-06$

4 Simulation experiment of similarity detection of science fiction painting

4.1 Experimental setup

We conduct simulation verification of the similarity detection method of science fiction painting. Firstly, MISSA-GP-TM is used to extract the target image from the science fiction painting to be detected. Secondly, pHash is used to detect the similarity of the matching results of science fiction painting. It is compared with gauss pyramid algorithm [1] and three algorithms PSO, SSA and CSSA that perform well on the CEC2017 benchmark function. In order to reflect the fairness of the test results, the key parameters of the experiment are set uniformly. P is set to 200, T_{max} is set to 100, dim is set to 2, K is set to 4, and m is set to 5. The specific parameter settings of each algorithm are consistent with Table 6, T_1, T_2 and a

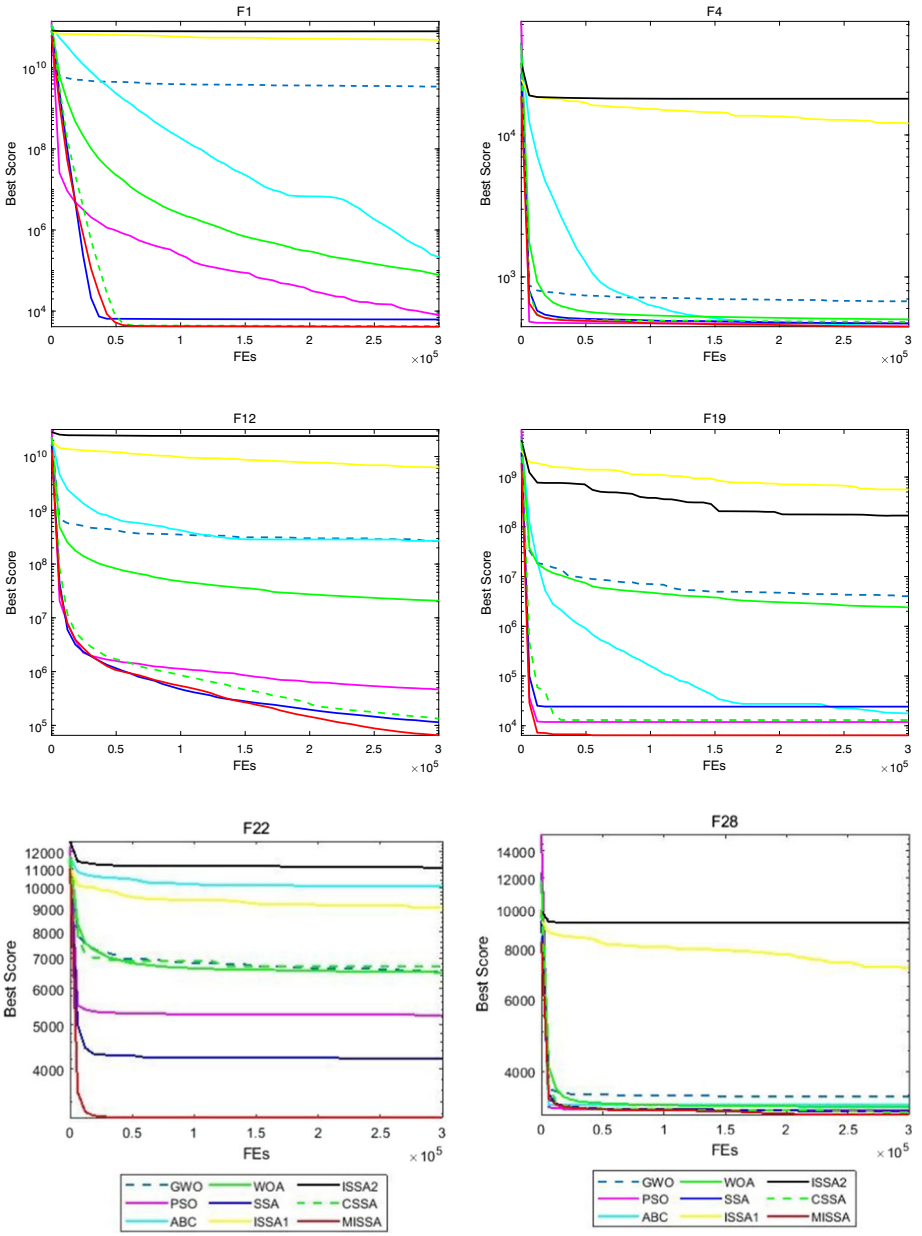

Fig. 3 Convergence analysis of different groups of functions

are adjusted to 10, 90 and 0.2 respectively in MISSA. Each method is run independently 50 times, and the average of each method is recorded as the final result. The simulation experiments are conducted on AMD Ryzen 5 4600H with Radeon Graphics CPU, 16G RAM (3200 MHz), and Windows 11 operating system, and the simulation software is MATLAB R2018a. Figure 5 shows two science fiction paintings with similar visual senses.

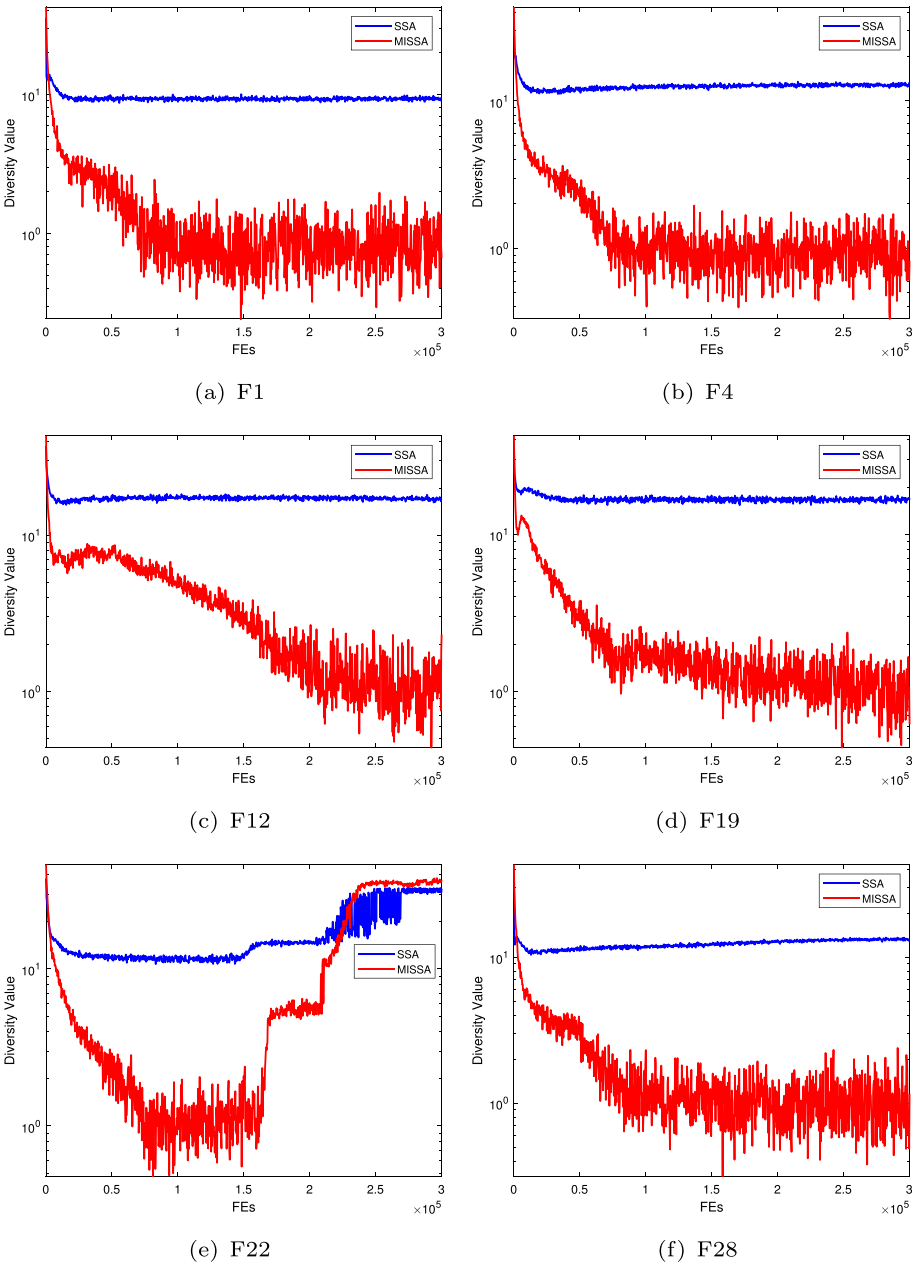

Fig. 4 Analysis of the population diversity between SSA and MISSA

As can be seen from Fig. 5, the two science fiction paintings have similar content in general, with only slight differences in brightness, color and several details. The overall similarity between the two science fiction paintings can be detected by pHash at 84.38%. In order to reduce the impact of non-major content on detection results, this paper selects

(a) (b)

Fig. 5 Comparison of similar science fiction paintings

four regions of interest in Fig. 5(b) as the template image, and then uses Fig. 5(b) as the science fiction painting to be detected, and extracts the target image. Figure 6 shows the science fiction painting to be detected and the template images of different sizes. For each group of images, hierarchical matching of GP-TM is used to calculate the matching time and similarity of each group of images, which can be used as the reference of other detection methods.

4.2 Experimental results

4.2.1 Comparison of running time

Table 9 shows the comparison of the time used by the GP-TM, PSO-GP-TM, SSA-GP-TM, CSSA-GP-TM and MISSA-GP-TM algorithms to locate the target image on template images with different sizes.

It can be seen from Table 9 that GP-TM has the longest average running time under different template sizes, which is about 1.9s in general. However, through the optimization of swarm intelligence optimization algorithm, the running time of GP-TM is greatly improved. PSO-GP-TM is about 1s shorter overall at size 123 $\times$ 142 (pix), 203 $\times$ 182 (pix) and 245 $\times$ 268 (pix), and only at size 206 $\times$ 217 (pix) is the average running time longer than GP-TM. However, SSA-GP-TM, CSSA-GP-TM and MISSA-GP-TM have a more significant improvement effect in time consumption, with an average running time of about 0.5s on the whole. It is worth noting that under the same template size, the running time of MISSA-GP-TM is the shortest compared with the other two methods. Therefore, our proposed MISSA-GP-TM algorithm has strong real-time performance and high computational efficiency, and can greatly reduce the running time of matching.

4.2.2 Comparison of similarity

Before similarity detection, the template matching method is used to search and locate the location of the target image in the science fiction painting to be detected. Figure 7 shows the final positioning results of five template matching algorithms in the science fiction painting to be detected, which are GP-TM, PSO-GP-TM, SSA-GP-TM, CSSA-GP-TM and MISSA-GP-TM from top to bottom.

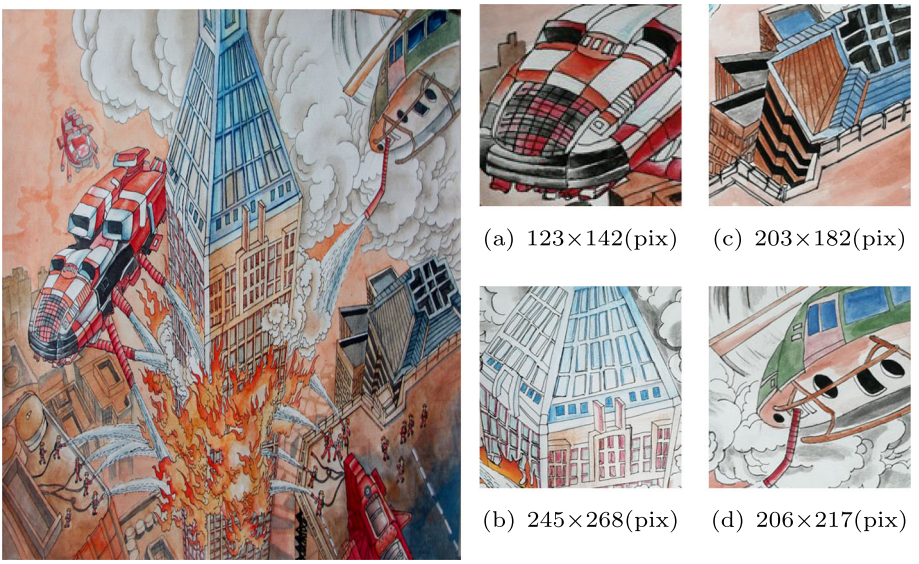

Fig. 6 Science fiction painting to be detected (left) and template images with four different sizes (right)

As can be seen from Fig. 7, SSA-GP-TM, CSSA-GP-TM and MISSA-GP-TM can all achieve the same matching result of GP-TM in a no-noise environment. However, PSO-GP-TM has poor matching results under the size 123×142 (pix) and 203×182 (pix), and cannot locate the most accurate position in the science fiction painting to be detected. In this paper, pHash is selected as the similarity measurement index, and the similarity less than 84.375% is generally judged to be dissimilar. The data in Table 10 shows that, after detection by the GP-TM method without noise, the average similarity between the template images of size 123×142 (pix), 203×182 (pix), 245×268 (pix) and 206×217 (pix) and the target images extracted from the science fiction painting to be detected is 85.94%, 89.06%, 95.31% and 85.94% respectively. Four groups of images can be judged to be similar. The similarity detection results of SSA-GP-TM, CSSA-GP-TM and MISSA-GP-TM are the same as those of GP-TM, indicating that these three template matching methods can accurately locate the location of the target image in the science fiction painting to be detected

4.2.3 Robustness comparison

In order to verify the anti-noise performance of each detection method, this paper adds Gaussian white noise with mean of 0 and variance of $0.01 \sim 0.1$ into the science fiction

Table 9 Comparison of the average time for matching on template images with different sizes (unit: s)

Algorithms	$123 \times 142(pix)$	$203 \times 182(pix)$	$245 \times 268(pix)$	$206 \times 217(pix)$
GP-TM	2.0249	1.9478	1.7704	1.8731
PSO-GP-TM	1.0337	0.7769	0.5971	2.5616
SSA-GP-TM	0.6977	0.4654	0.5587	0.4468
CSSA-GP-TM	0.6286	0.5082	0.6665	0.4670
MISSA-GP-TM	0.4639	0.3533	0.4951	0.4235

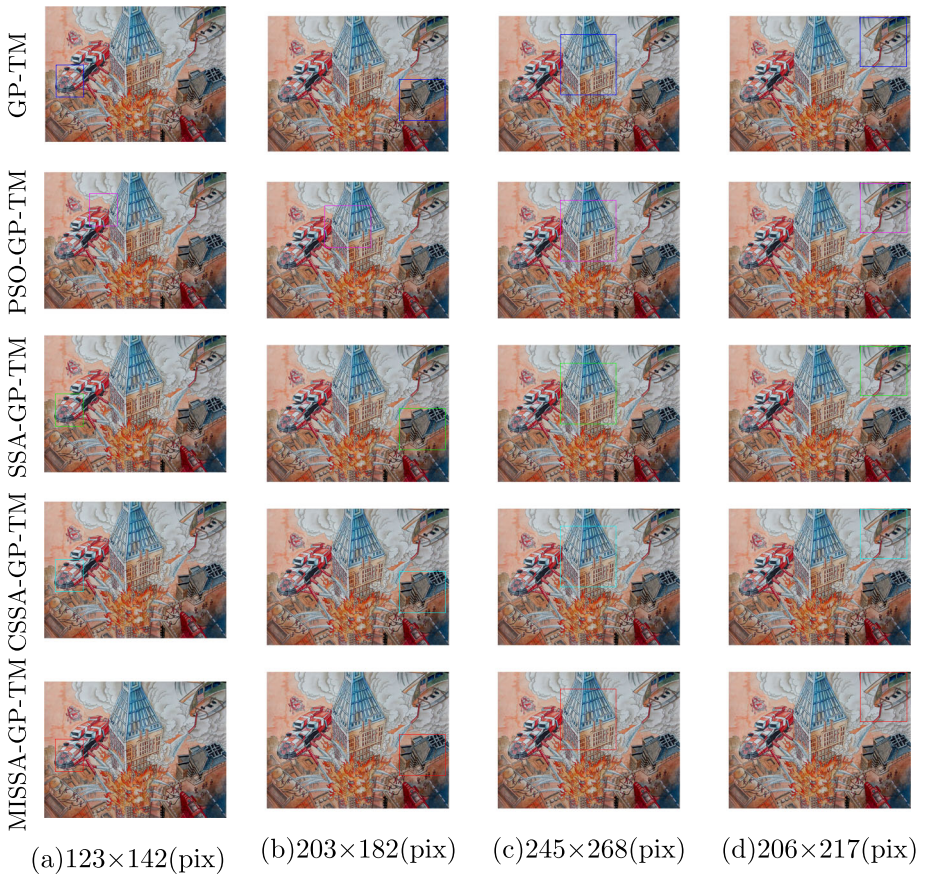

Fig. 7 Localization results of 5 template matching algorithms on template images with different sizes

painting to be detected. Figure 8 is the radar chart of similarity comparison of four groups of target images under different levels of noise. It can be seen from Fig. 8 that, compared with the case without noise in Table 10, different levels of noise affect the final detection result of GP-TM. In the process of target image extraction, due to the influence of different degrees of noise, there are many outstanding mutual information peaks, and even many peaks are beyond the peak of the correct position, so that GP-TM cannot find the

Table 10 Comparison of similarity detection results without noise

Algorithms	$123 \times 142(pix)$	$203 \times 182(pix)$	$245 \times 268(pix)$	$206 \times 217(pix)$
GP-TM	85.94%	89.06%	95.31%	85.94%
PSO-GP-TM	84.06%	84.69%	95.08%	85.25%
SSA-GP-TM	85.94%	89.06%	95.31%	85.94%
CSSA-GP-TM	85.94%	89.06%	95.31%	85.94%
MISSA-GP-TM	85.94%	89.06%	95.31%	85.94%

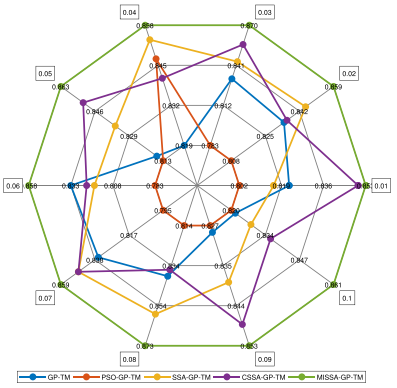

(a) Anti-noise performance on the 123 ×142 (pix)

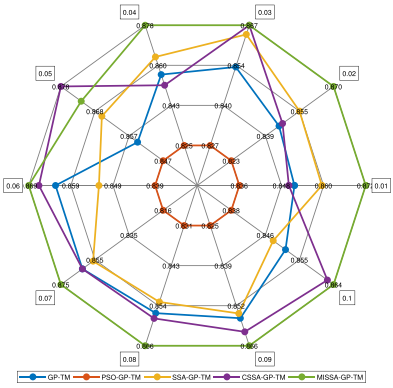

(b) Anti-noise performance on the 203×182 (pix)

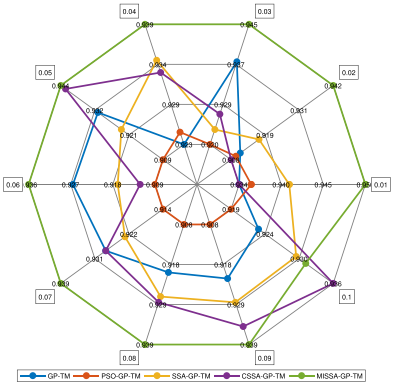

(c) Anti-noise performance on the 245×268 (pix)

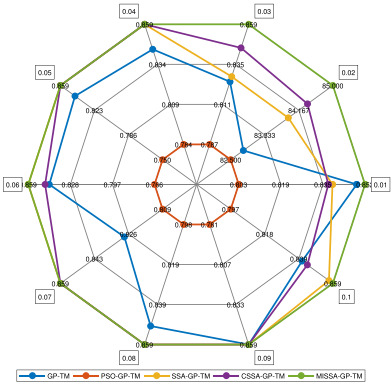

(d) Anti-noise performance on the 206×217 (pix)

Fig. 8 Comparison of noise resistance on template images with different sizes

correct position in the science fiction painting to be detected, resulting in mismatching that affects the final detection result. In addition, we find that adding Gaussian white noise to the science fiction painting to be detected has the greatest impact on PSO-GP-TM, mainly because its image matching accuracy is not high in the absence of noise, and the appearance of noise only leads to a higher probability of mismatching. It can be clearly seen from the four radar charts that the area covered by MISSA-GP-TM is the largest, which means that the overall anti-noise performance of MISSA-GP-TM is optimal. MISSA-GP-TM performs worse than CSSA-GP-TM only on the size 203 × 182 (pix) with variance of 0.05 and the size 245 × 268 (pix) with variance of 0.1, while the detection results on the size 206 × 217 (pix) with variance of 0.03 ∼ 0.1 are the same as those without noise. These results fully demonstrate that MISSA-GP-TM has strong robustness under the condition of ensuring the accuracy and real-time of matching, and can provide a stable performance and high accuracy similarity detection method for more complex science fiction painting in the future.

4.3 Discussion

The image matching problem can be considered as a single-objective optimization problem, and the swarm intelligence optimization algorithm has great potential to reduce the matching time. As shown in Table 9, the average running time of the GP-TM based on the swarm intelligence optimization algorithm at different template sizes is substantially reduced compared to the original GP-TM. Furthermore, the maximum potential of the algorithm can be stimulated by improving the swarm intelligence optimization algorithm. It can be seen from Table 9 that the running time of MISSA-GP-TM (a variant of SSA-GP-TM) is further improved at the same template size and it has the shortest running time compared to other algorithms. Although such optimization methods can significantly reduce the matching time, they tend to converge prematurely due to the ineffective search strategy, which leads to suboptimal (or even incorrect) matching. As observed in Fig. 7 and Table 10, the similarity detection results of SSA-GP-TM, CSSA-GP-TM, and MISSA-GP-TM are the same as GP-TM in a noise-free environment, and all of them are able to accurately locate the position of the target image in the science fiction painting to be detected, while the matching results of PSO- GP-TM are poor. Meanwhile, the robustness of the algorithm is also of concern. As can be seen in Fig. 8, different levels of noise affect the final detection results of GP-TM compared to the noise-free case in Table 10. However, we can clearly see from the four sets of radar plots that the area covered by MISSA-GP-TM is the largest, which means that MISSA-GP-TM is less affected by noise and its overall noise immunity is optimal. All the above experimental results show that MISSA-GP-TM achieves the best balance between matching accuracy and computational cost, and has strong robustness compared with other similar methods. It also fully illustrates the success of the hybrid search strategy based on the step function, the multi-stage dynamic control factor, and the food search strategy based on the Logistic model introduced in the sparrow search algorithm.

5 Conclusion

In order to make up for the gap in the similarity detection of science fiction painting, this paper proposes a template matching algorithm based on multi-strategy improved sparrow search algorithm and Gaussian pyramid, which is applied to the extraction of target images of science fiction painting. Compared with the sparrow search algorithm, the innovation of MISSA is mainly manifested in the hybrid search strategy based on step function in the position update stage of producer, multi-stage dynamic control of safety threshold, and the food search strategy based on Logistic model in the position update stage of scrounger. The ergodic matching at the top layer of the Gaussian pyramid is replaced by MISSA with strong global optimization ability. Therefore, the hierarchical matching strategy of the Gaussian pyramid can further improve the matching effect of science fiction painting with the assistance of MISSA. In the similarity detection part, pHash is selected as a measure of the similarity between the target image and the template image. The following main conclusions are obtained:

(1) The ablation experiment proves that the hybrid search strategy based on step function, the multi-stage dynamic control factor and the food search strategy based on the Logistic model can all provide effective help for the improvement of SSA. Through the analysis of the time complexity of the algorithm, we can see that the improved strategy proposed in this paper for SSA does not increase the time complexity of the algorithm.

(2) The results of Freidman test and Wilcoxon signed-rank test on the CEC2017 benchmark function show that, compared with peer algorithms, MISSA has stronger optimization ability in solving high-dimensional complex function problems. On the convergence curves of F1, F4, F12, F19, F22 and F28, MISSA has a faster convergence speed and can converge to a solution with higher accuracy.
(3) In the detection experiment of science fiction painting without noise, compared with GP-TM, PSO-GP-TM, SSA-GP-TM and CSSA-GP-TM, MISSA-GP-TM can accurately locate the position of the target image in the science fiction painting to be detected with the shortest average running time. Adding different degrees of Gaussian white noise to the science fiction painting to be detected for similarity detection, we can see from the four sets of radar charts that the impact on MISSA-GP-TM is the smallest, and its overall anti-noise performance is the best. This fully verifies that MISSA-GP-TM has strong applicability in the similarity detection of science fiction painting, and has strong robustness under the condition of ensuring accuracy and real-time matching.

Our future work focuses on the case of multi-objective region detection of science fiction paintings, and the algorithm in this paper is subsequently improved further, so as to enhance the practicality and applicability of the algorithm and make it better applied to the similarity detection of science fiction paintings. In addition, the initial parameters and positions of MISSA affect the final optimization results, which makes the optimization results of the algorithm more or less dependent on subjective experience, so finding a more objective initialization of the algorithm is the focus of our next algorithm improvement.

Acknowledgements This research did not receive any specific grant from funding agencies in the public, commercial, or not-for-profit sectors.

Data Availability All data generated or analysed during this study are included in this published article (and its supplementary information files).

Author Contributions Gang Chen: Conceptualization, Methodology, Data curation, Validation, Formal analysis, Software, Writing - original draft, Writing - review & editing. Donglin Zhu: Methodology, Writing - original draft, Supervision, Validation. Xiangyu Chen: Writing -review & editing.

Declarations

Competing interests The authors declare that they have no known competing financial interests or personal relationships that could have appeared to influence the work reported in this paper.

References

1. Adelson E, Anderson C, Bergen J, Burt P, Ogden J (1983) Pyramid methods in image processing. RCA engineer, 29
2. Berahmand K, Mohammadi M, Faroughi A, Mohammadiani RP (2022) A novel method of spectral clustering in attributed networks by constructing parameter-free affinity matrix. Clust Comput 25(2):869–888
3. Bunke H, Shearer K (1998) A graph distance metric based on the maximal common subgraph. Pattern Recogn Lett 19(3-4):255–259
4. Chang L, Wang RF, Zhang Y (2022) Decoding ssvep patterns from eeg via multivariate variational mode decomposition-informed canonical correlation analysis. Biomed Signal Process Control 71:103209
5. Chen G, Lin D, Chen F et al (2023) Image segmentation based on Logistic regression sparrow algorithm[J]. Journal of Beijing University of Aeronautics and Astronautics 49(3):636–646. in Chinese https://doi.org/10.13700/j.bh.1001-5965.2021.0268

6. Chen GG, Tang BR, Zeng XJ, Zhou P, Kang P, Long HY (2022) Short-term wind speed forecasting based on long short-term memory and improved bp neural network. Int J Electr Power Energy Syst 134:107365
7. Cuevas E, Echavarría A, Zaldívar D, Pérez-Cisneros M (2013) A novel evolutionary algorithm inspired by the states of matter for template matching. Expert Syst Appl 40(16):6359–6373
8. Derrac J, García S, Molina D, Herrera F (2011) A practical tutorial on the use of nonparametric statistical tests as a methodology for comparing evolutionary and swarm intelligence algorithms. Swarm Evol Comput 1(1):3–18
9. Gai JB, Zhong KY, Du XJ, Yan K, Shen JX (2021) Detection of gear fault severity based on parameter-optimized deep belief network using sparrow search algorithm. Measurement 185:110079
10. Ganti PK, Naik H, Barada MK (2021) Environmental impact analysis and enhancement of factors affecting the photovoltaic (pv) energy utilization in mining industry by sparrow search optimization based gradient boosting decision tree approach. Energy 122561
11. García S, Fernández A, Luengo J, Herrera F (2010) Advanced nonparametric tests for multiple comparisons in the design of experiments in computational intelligence and data mining: experimental analysis of power. Inform Sci 180(10):2044–2064
12. Girshick R, Donahue J, Darrell T, Malik J (2014) Rich feature hierarchies for accurate object detection and semantic segmentation. In: Proceedings of the IEEE conference on computer vision and pattern recognition (CVPR)
13. González A, Cuevas E, Fausto F, Valdivia A, Rojas R (2017) A template matching approach based on the behavior of swarms of locust. Appl Intell 47(4):1087–1098
14. Jiang F, Han XY, Zhang WY, Chen GC (2021) Atmospheric pm2. 5 prediction using deepar optimized by sparrow search algorithm with opposition-based and fitness-based learning. Atmosphere 12(7):894
15. Kang LW, Hsu CY, Chen HW, Lu C-S, Lin CY, Pei SC (2011) Feature-based sparse representation for image similarity assessment. IEEE Trans Multimed 13(5):1019–1030
16. Karaboga D, Akay B (2009) A comparative study of artificial bee colony algorithm. Appl Math Comput 214(1):108–132
17. Karaboga D, Basturk B (2008) On the performance of artificial bee colony (abc) algorithm. Appl Soft Comput 8(1):687–697
18. Kathiroli P, Selvadurai K (2021) Energy efficient cluster head selection using improved sparrow search algorithm in wireless sensor networks. Journal of King Saud University-Computer and Information Sciences
19. Kennedy J, Eberhart R (1995) Particle swarm optimization. In: Proceedings of ICNN'95 - international conference on neural networks, vol 4, pp 1942–1948
20. Li B, Gong LG, Li Y (2014) A novel artificial bee colony algorithm based on internal-feedback strategy for image template matching. Scientific World Journal 2014
21. Liang QK, Chen B, Wu HN, Ma CY, Li SY (2021) A novel modified sparrow search algorithm with application in side lobe level reduction of linear antenna array. Wirel Commun Mob Comput, 2021
22. Liu GY, Shu C, Liang ZW, Peng BH, Cheng LF (2021) A modified sparrow search algorithm with application in 3d route planning for uav. Sensors 21(4):1224
23. Liu WB, Wang ZD, Yuan Y, Zeng NY, Hone K, Liu XH (2021) A novel sigmoid-function-based adaptive weighted particle swarm optimizer. IEEE Trans Cybern 51(2):1085–1093
24. Liu XR, Wang ZJ, Wang L, Huang C, Luo X (2021) A hybrid rao-nm algorithm for image template matching. Entropy 23(6):678
25. Meng XB, Liu Y, Gao XZ, Zhang HZ (2014) A new bio-inspired algorithm: chicken swarm optimization. In: International conference in swarm intelligence. Springer, pp 86–94
26. Mirjalili S, Lewis A (2016) The whale optimization algorithm. Adv Eng Softw 95:51–67
27. Mirjalili S, Mirjalili SM, Lewis A (2014) Grey wolf optimizer. Adv Eng Softw 69(3):46–61
28. Mohamed AAA, Hassan SA, Hemeida AM, Alkhalaf S, Mahmoud MMM, Eldin AMB (2020) Parasitism–predation algorithm (ppa): a novel approach for feature selection. Ain Shams Eng J 11(2):293–308
29. Nasiri E, Berahmand K, Li Y (2022) Robust graph regularization nonnegative matrix factorization for link prediction in attributed networks. Multimed Tools Applic, 1–24
30. Ouyang C, Qiu YX, Zhu DL (2021) Adaptive spiral flying sparrow search algorithm. Sci Program, 2021
31. Raghav LP, Kumar RS, Raju DK, Singh AR (2022) Analytic hierarchy process (ahp)–swarm intelligence based flexible demand response management of grid-connected microgrid. Appl Energy 306:118058
32. Rostami M, Berahmand K, Nasiri E, Forouzandeh S (2021) Review of swarm intelligence-based feature selection methods. Eng Appl Artif Intell 100:104210
33. Shen Y FXWX (2022) A multi-scale sine cosine algorithm for optimization problems. Control and Decision, 1–10

34. Song CG, Yao LH, Hua CY, Ni QH (2021) A novel hybrid model for water quality prediction based on synchrosqueezed wavelet transform technique and improved long short-term memory. J Hydrol 603:126879
35. Swain MJ, Ballard DH (1991) Color indexing. Int J Comput Vis 7(1):11–32
36. Tian ZD, Chen H (2021) A novel decomposition-ensemble prediction model for ultra-short-term wind speed. Energy Convers Manage 248:114775
37. Turgut MS, Turgut OE, Eliiyi DT (2020) Island-based crow search algorithm for solving optimal control problems. Appl Soft Comput 90:106170
38. Umeyama S (1988) An eigendecomposition approach to weighted graph matching problems. IEEE Trans Pattern Anal Mach Intell 10(5):695–703
39. Wang P, Zhang Y, Yang H (2021) Research on economic optimization of microgrid cluster based on chaos sparrow search algorithm. Comput Intell Neurosci 2021
40. Wang YN, Wang W, Tao GC, Li HL, Zheng Y, Cui JH (2022) Optimization of the semi-sphere vortex generator for film cooling using generative adversarial network. Int J Heat Mass Transf 183:122026
41. Wu CY, Fu XS, Pei JK, Dong ZG (2021) A novel sparrow search algorithm for the traveling salesman problem. IEEE Access 9:153456–153471
42. Wu YH, Sun LQ, Sun XB, Wang BN (2021) A hybrid xgboost-issa-lstm model for accurate short-term and long-term dissolved oxygen prediction in ponds. Environ Sci Pollut Res, 1–18
43. Xiong Q, Zhang XM, He SB, Shen J (2021) A fractional-order chaotic sparrow search algorithm for enhancement of long distance iris image. Mathematics 9(21):2790
44. Xue JK, Shen B (2020) A novel swarm intelligence optimization approach: sparrow search algorithm. Syst Sci Control Eng 8(1):22–34
45. Yan SQ, Yang P, Zhu DL, Zheng WL, Wu FX (2021) Improved sparrow search algorithm based on iterative local search. Comput Intell Neurosci, 2021
46. Yang L, Li Z, Wang DS, Miao H, Wang ZB (2021) Software defects prediction based on hybrid particle swarm optimization and sparrow search algorithm. IEEE Access 9:60865–60879
47. Zamani H, Nadimi-Shahraki MH, Gandomi AH (2019) Ccsa: Conscious neighborhood-based crow search algorithm for solving global optimization problems. Appl Soft Comput 85:105583
48. Zauner C (2010) Implementation and benchmarking of perceptual image hash functions
49. Zhang CL, Ding SF (2021) A stochastic configuration network based on chaotic sparrow search algorithm. Knowl-Based Syst 220:106924
50. Zhang JN, Xia KW, He ZP, Yin ZX, Wang SJ (2021) Semi-supervised ensemble classifier with improved sparrow search algorithm and its application in pulmonary nodule detection. Math Probl Eng, 2021
51. Zhao WG, Zhang ZX, Wang LY (2020) Manta ray foraging optimization: an effective bio-inspired optimizer for engineering applications. Eng Appl Artif Intell 87:103300
52. Zhao D, Liu L, Yu F, Heidari AA, Wang M, Liang G, Muhammad K, Chen H (2021) Chaotic random spare ant colony optimization for multi-threshold image segmentation of 2d kapur entropy. Knowl-Based Syst 216:106510
53. Zhou SH, Xie H, Zhang CC, Hua YZ, Zhang WH, Chen Q, Gu GH, Sui XB (2021) Wavefront-shaping focusing based on a modified sparrow search algorithm. Optik 244:167516
54. Zhu YL, Yousefi N (2021) Optimal parameter identification of pemfc stacks using adaptive sparrow search algorithm. Int J Hydrogen Energy 46(14):9541–9552

Affiliations

Gang Chen[1] · Donglin Zhu[2] · Xiangyu Chen[1]

Donglin Zhu
6920190624@mail.jxust.edu.cn

Xiangyu Chen
201127012@fzu.edu.cn

[1] College of Physics and Information Engineering, Fuzhou University, Fuzhou, 350108, China

[2] School of Information Engineering, Jiangxi University of Science and Technology, Ganzhou, 341000, China